

Unravelling technological behaviors through core reduction intensity. The case of the early Protoaurignacian assemblage from Fumane Cave

Diego Lombao^{a,b,*,1}, Armando Falcucci^{c, **,1}, Elena Moos^c, Marco Peresani^{d,e}

^a GEPN-AAT, Departamento Historia, Facultade de Xeografía e Historia, USC, Praza da Universidade 1, 15782, Santiago de Compostela, Spain

^b Institut Català de Paleoecología Humana i Evolució Social (IPHES-CERCA), Zona Educacional 4, Campus Sescelades URV (Edifici W3), 43007, Tarragona, Spain

^c Department of Geosciences, Prehistory and Archaeological Sciences Research Unit, Eberhard Karls University of Tübingen, Tübingen, Germany

^d Department of Humanities, Prehistoric and Anthropological Sciences Unit, University of Ferrara, Ferrara, Italy

^e Institute of Environmental Geology and Geoengineering, National Research Council, Milano, Italy



ARTICLE INFO

Keywords:

Lithic technology
Experimental Archaeology
Reduction Intensity
Volumetric Reconstruction Method
Scar Density Index
Protoaurignacian

ABSTRACT

This paper investigates core reduction intensity in the early Protoaurignacian lithic assemblage from Fumane Cave in northeastern Italy. Reduction intensity serves as a key tool to characterize blank selection strategies, raw material management, and the variability of knapping strategies throughout the reduction sequence by reconstructing the operatory field of core assemblages. Finally, it also aids in addressing the relationship between blades and bladelets, providing valuable insights into the behavioral and chrono-cultural significance of laminar productions within the Aurignacian technocomplex. To achieve these research goals, experimental work employing 3D scanning technology was conducted. This facilitated the comparison of different methods and variables for measuring reduction intensity, including the percentage of non-cortical surface, the Scar Density Index (SDI), and a novel adaptation of the Volumetric Reconstruction Method (VRM). Results demonstrate the effectiveness and potential of adapting the VRM for the study of reduction intensity in Upper Paleolithic laminar cores, and the provided R scripts and datasets will enable this method to be applied to other contexts with minimal need for modification to the workflow. Analysis of reduction intensity measures applied to the Protoaurignacian assemblage from Fumane Cave reveals slight variations based on factors such as the abundance and proximity of selected raw materials for blank production. Notably, the most prevalent raw material variety, the Maiolica, yields a higher number of less reduced cores, while reduction levels across all cores discarded at the site remain relatively high. The observed variability in the operatory field and the interrelation between blade and bladelet productions underscore the complexity and flexibility of Protoaurignacian behavior. This inherent complexity challenges any definitive separation between the operatory fields of blade and bladelet productions. These findings are particularly important to emphasize the importance of considering reduction intensity when examining technological variability and human behavior in Aurignacian studies. The proposed adaptation of the VRM and the effective combination with other measures of reduction, promises to allow future research to incorporate reduction intensity as a vital temporal component within studies on stone tool production. This integration offers a pathway to enhancing our understanding of the adaptive behaviors exhibited by *Homo sapiens* across diverse ecological settings and provides a clearer framework for better framing the development of the Upper Paleolithic.

* Corresponding author. GEPN-AAT, Dpto. Historia, Facultade de Xeografía e Historia, USC, Praza da Universidade 1, 15782, Santiago de Compostela, Spain.

** Corresponding author.

E-mail addresses: diego.lombao@usc.es (D. Lombao), armando.falcucci@uni-tuebingen.de (A. Falcucci).

¹ These authors have contributed equally.

<https://doi.org/10.1016/j.jas.2023.105889>

Received 6 August 2023; Received in revised form 27 October 2023; Accepted 30 October 2023

Available online 10 November 2023

0305-4403/© 2023 The Authors. Published by Elsevier Ltd. This is an open access article under the CC BY-NC license (<http://creativecommons.org/licenses/by-nc/4.0/>).

1. Introduction

1.1. Foreword, definition, and geography

The Aurignacian is essential to the discussion surrounding the development of the Upper Paleolithic and the associated dispersal of modern humans across Europe. A growing body of data suggests that this biocultural process was the result of multiple migrations, some of which might have been very old and less successful (Benazzi et al., 2011; Harvati et al., 2019; Hublin et al., 2020; Slimak et al., 2022). By 42 thousand years ago, however, Aurignacian assemblages are found all along the Mediterranean basin and Central Europe, making this technocomplex the most solid archaeological evidence for the definitive spread of *Homo sapiens* populations (Benazzi et al., 2011, 2015; Davies, 2007; Frouin et al., 2022; Higham et al., 2014; Hoffecker, 2009; Hublin, 2015; Mellars, 2006; Teyssandier et al., 2010; Wood et al., 2014). The association between Aurignacian assemblages and *Homo sapiens* remains is solid (Dujardin, 2001; Verna et al., 2012). Most of the findings relate to teeth (Bailey et al., 2009), among which two incisors recovered at Bombrini Shelter and Fumane Cave stand out for having been found in the lowermost Protoaurignacian units (Benazzi et al., 2015).

The earliest manifestations of the Aurignacian are statistically constrained between 44 and 42 ky cal BP and are mainly concentrated along Mediterranean Europe and the Danube Basin (Barshay-Szmidt et al., 2013, 2018; Conard and Bolus, 2003, 2008; Davis and Hedges, 2008; Douka et al., 2012; Falcucci et al., 2017; Falcucci and Peresani, 2018; Haws et al., 2020; Higham et al., 2012; Marciani et al., 2020; Nigst et al., 2014; Szmidt et al., 2010; Teyssandier and Zilhão, 2018; Valdes and Bischoff, 1989; Villaverde et al., 2021; Wood et al., 2014). The seemingly marked differences in the material culture between these two macro-regions and the very old radiocarbon dates obtained in the Swabian Jura (southwestern Germany), led a few authors to suggest that modern humans might have followed different cultural trajectories during their expansion across Europe (Conard and Bolus, 2006; Davies, 2007; Higham et al., 2012) contra (Chu, 2018; Zilhão and D'Errico, 2003).

Since the discovery of the eponymous site, Abri d'Aurignac, by Édouard Lartet in the middle of the 19th century (see Bon, 2002a), the Aurignacian has been the subject of an increasing number of studies (Bon, 2002a; de Sonneville-Bordes, 1960, 1983; Delporte, 1991; Demars, 1992; Peyrony, 1933). These studies have allowed scholars to propose a chrono-cultural division of the technocomplex into four main phases (see Bordes, 2005; Teyssandier and Zilhão, 2018). The first two phases (i.e., the Protoaurignacian and the Early Aurignacian) have received most of the attention (Bon et al., 2010; Teyssandier et al., 2010), mainly due to the debate surrounding the arrival of modern humans in Europe and the associated behavioral adaptations, reflected also by an increase in the use of ornamental objects made from seashells, bone and antler tools, as well as mineral pigments (d'Errico et al., 2012; Stiner, 1999; Vanhaeren and D'Errico, 2006), among other behavioral traits.

1.2. Lithic reduction patterns of reference

The Aurignacian has been divided mainly based on technological criteria. Recent assessments have focused on the technological features of blade and bladelet productions. Among them, the most discussed elements are core preparation and maintenance, the independence or continuity in the production of blades and bladelets, and the further modification of these blanks through retouching (Bon et al., 2010; Teyssandier and Zilhão, 2018). In this framework, the Protoaurignacian is traditionally identified by evidence to produce blades and bladelets within a continuous reduction sequence, as opposed to the Early Aurignacian, where blade and bladelet productions involve independent core reduction sequences. In the Protoaurignacian, thus, there would be a less marked anticipation of different needs, with

products mainly devoted to domestic and hunting activities being produced in the same timeframe (Bon, 2002b, 2005, 2006; Bon and Bodu, 2002). Blades, in particular, would be obtained in the early stages of core reduction, an observation supported by the near absence of blade cores in most Protoaurignacian assemblages, as well as the morphological affinity and dimensional continuity across laminar blanks (Arrizabalaga and Altuna, 2000; Bon, 2002b; Maillo-Fernández, 2005; Santamaría, 2012; Teyssandier, 2007; Tsanova et al., 2012).

In the early stages of the Aurignacian, core technology exhibits a wide range of knapping strategies and a certain flexibility in the preparation phases, which however are not as standardized as in following stages of the Upper Paleolithic (e.g., the Gravettian: (Otte, 2013) and references therein). Interestingly, Early Aurignacian blade cores in Aquitaine and the Swabian Jura are frequently characterized by platform faceting; a technical solution aimed at extracting robust blades. Faceting is instead virtually absent in the Protoaurignacian, with little evidence towards its later stages (e.g., Falcucci et al., 2020). However, the most defining difference between Proto- and Early Aurignacian assemblages is represented by the high frequency in the use of carinated technology in the latter (Dinnis et al., 2019; Teyssandier and Zilhão, 2018). On the other hand, the presence and importance of carinated cores in the Protoaurignacian is a rather debated topic, which has sparked an intense debate among scholars regarding the meaning and validity of this chrono-cultural framework and its applicability to a vast geographic region (Bataille et al., 2020; Dinnis et al., 2019).

In this regard, neither the nature of these phases (i.e., cultural or functional; see discussion in Tafelmaier (2017)), nor the characteristics that define each subphase within the Aurignacian macro-group are free from controversy (Bataille, 2017). In some Protoaurignacian sites, such as at Fumane Cave, the linear continuity in the production of blades and bladelets within the same reduction sequence has been questioned in its most orthodox definition (Falcucci et al., 2017; Falcucci and Peresani, 2018). The existence of two independent production systems seems in fact to be quite common and widespread across regions. This is, for instance, the case at Mochi and Bombrini in northwestern Italy (Bertola et al., 2013; Douka et al., 2012; Riel-Salvatore and Negrino, 2018), La Viña, Labeko Koba, and Isturitz in Cantabrian Spain (Normand et al., 2008; Santamaría, 2012; Tafelmaier, 2017), as well as in the western margins of the Mediterranean Basin, such as at Arbreda (Ortega-Cobos et al., 2005). This combined evidence led some authors to argue that the independence of blade and bladelet productions is not the most reliable proxy to discuss the cultural variation within the Aurignacian technocomplex (Bataille, 2017; Falcucci et al., 2017; Tafelmaier, 2017).

It has been for instance argued that a few cores discarded at sites such as Arbreda, La Viña, and Fumane show clear evidence of exclusive blade production (Bertola et al., 2013; Falcucci et al., 2017; Falcucci and Peresani, 2018; Ortega-Cobos et al., 2005; Santamaría, 2012), and that blades and/or blade cores might have been exported from the site following differential strategies in relation to human mobility (Tafelmaier, 2017). Furthermore, the morphological affinities between blades and bladelets may not necessarily represent a continuity in the reduction sequence. Both production systems can share similar knapping strategies, operatory fields, and similar technical solutions, thus resulting in similar products. In this regard, Falcucci et al. (2022) statistically quantified the marked similarity between blades and bladelets using a three-dimensional geometric morphometric approach. The authors noticed that most of the differences, linked to the allometric variation of blanks, are related to the use of specific maintenance and initialization operations carried out on bladelet cores, by means of the extraction of wide and often plunging blades, and the progressive extraction of blanks with convergent edges as production moved towards more advanced stages of reduction. It should be also noticed that the dimensional continuity identified at Fumane between blades and bladelets does not seem to be a very reliable argument to discuss dimensional continuity since blanks can be obtained from cores with quite different sizes (Falcucci et al., 2017). Finally, the continuity in the dimensions of blades and

bladelets could be well affected by factors such as the differential transport of products and raw materials in the complex framework of mobility strategies adopted by foraging groups, calling for more discussions on a case-by-case basis (Tafelmaier, 2017).

Despite the magnitude of this debate, we have identified two factors that clearly limit our understanding of the Protoaurignacian. First, extensive lithic refitting programs have not been carried out to empirically confirm or reject the existence of a systematic transfer between the production of blades and bladelets. Isolated examples exist, such as for instance a partially refitted blade core recovered in the earliest Protoaurignacian unit at Fumane Cave (Falcucci et al., 2017), although results cannot be generalized. Second, although to date the reduction intensity has been considered as an influencing factor in a certain qualitative way, based mainly on the degree of exhaustion of the cores, this issue has not been addressed by measuring the reduction intensity from a quantitative standpoint, thus amenable to statistical testing. We argue that quantifying the reduction intensity of an assemblage can provide key information about critical aspects of human behavior and assemblage formation processes (see Schiffer, 1987).

1.3. A critical review of reduction intensity studies and research objectives

Reduction intensity is a pivotal element for studying the adaptation of humans group to their environment, such as in terms of management of raw materials in relation to availability, abundance, and proximity of resources, as well as for understanding the different strategies for their acquisition, transport, use, and discard (e.g., Andrefsky, 1994; Blades, 2003; Carr and Bradbury, 2011; Kuhn, 1991; Lombao et al., 2023b; Morales, 2016; Nelson, 1991; Rolland and Dibble, 1990; Shott and Silsbee, 2005, 2004). Furthermore, reduction intensity is a crucial element for parsimoniously exploring technological variability. A few authors have already stressed how a typological approach to core classification does not allow exploration of knapping strategies and their relationship with each other within a solid diachronic component, which is at the base of each reductive activity (e.g., Dibble, 1995a; Lombao, 2021; Lombao et al., 2023b; Rabanal, 2016). A well-framed diachronic approach would allow for a more efficient and reliable reconstruction of the operatory field of human groups, that is, the set of technical strategies and decisions involved in the process of stone tool production (Guilbaud, 1993, 1995).

Taking these aspects into account, we emphasize that reduction intensity is crucial for more parsimoniously addressing Protoaurignacian technological behavior, and researchers need to make additional efforts to explore these aspects. The main challenge that we face is related to the fact that no studies specifically tackle reduction intensity in blade and bladelet cores. This is a major research gap if contrasted with the proliferation of methods aimed at quantifying the reduction of blanks obtained through laminar knapping strategies. A notable example is a study on the reduction of backed blades (Muller et al., 2018), among several others (e.g., Bustos-Pérez and Baena, 2019; Eren et al., 2005; Eren and Sampson, 2009; Kuhn, 1990; Morales et al., 2015). On the other hand, quite a few “generalists” methods oriented at measuring core reduction intensity exist. They tend to cover a wide range of knapping methods using technological proxies that correlate with reduction intensity, such as the Scar Density Index (SDI) developed by Clarkson (2013). Other methods are instead oriented toward the volumetric reconstruction of the original raw material nodules (Douglass et al., 2018; Lombao et al., 2020).

In the specific case of Protoaurignacian blade and bladelet technologies, the method proposed by Douglass et al. (2018) has some limitations that hinder its successful application. For example, the number of flaking surfaces cannot be easily determined in semi-tournant cores, as a clear-cut limit between flaking surfaces is difficult to determine, which could also affect the inter-rater replicability of analytical observations. For the same reason, it is also challenging to quantify the number of convergences between flaking surfaces. As for the Volumetric

Reconstruction Method (VRM) (Lombao et al., 2020), its original application was not aimed at quantifying reduction intensity in laminar technological systems of the Upper Paleolithic, but it rather focused on less standardized technologies typical of the Lower Paleolithic (Cueva-Temprana et al., 2022; Lombao et al., 2023c). Moreover, its application was centered on cobbles with ellipsoidal morphologies, thus excluding those raw materials characterized by irregular morphologies, such as blocks and chunks. The VRM has proven to be a highly effective method that allows to quantify reduction intensity not only on an entire assemblage, but also on a case-by-case level. Moreover, the method derives its data from a combination of 3D model analysis of cores and metric measurements of the entirety of the blank assemblage associated with these cores, thus greatly increasing the statistical reliability of the observations.

To overcome the existing limitations of the VRM, here, we develop an adaptation of the approach focused on the quantification of reduction intensity, understood as the percentage of extracted core volume, across unidirectional blade and bladelets cores. We will first conduct an experimental evaluation of different reduction intensity methods and variables, such as the percentage of non-cortical surface, the SDI, the here proposed methodological adaptation of the VRM, and other aspects such as the number of flaking surfaces and striking platforms, as well as the mean knapping angles. This evaluation will allow us to assess the performance of the VRM and discriminate the most appropriate combination of methods for studying reduction intensity in blade and bladelets cores. Subsequently, we will quantify reduction intensity in one of the most important Protoaurignacian assemblages, Fumane Cave in northeastern Italy (Bartolomei et al., 1992), using a recently published open-access repository of 3D meshes of core types (Falcucci and Persani, 2023) and the technological dataset from Falcucci et al. (2017).

Our main goals are: 1) to characterize blank selection strategies and raw material management; 2) to study the variability of reduction strategies throughout the reduction process, thus aiming at reconstructing the operatory field of the core assemblage and, 3) to address the issue of the independence or continuity of blade and bladelet productions to help clarifying the behavioral and chrono-cultural meaning of this technological feature. Overall, we will assess the reduction intensity of all cores involved in the production of blades and bladelets to provide new insights into the technological behavior of Protoaurignacian foragers settled in the region.

2. Materials and methods

2.1. The experimental protocol

To test the applicability of the VRM to our case study, we designed an experimental protocol involving the reduction of laminar cores starting from nodules (both complete and fragmented) and slabs. The prior VRM experiment dealt with cores and tools on cobbles reduced using reduction procedures typical of Lower Paleolithic assemblages, which cannot be equated to the Upper Paleolithic. The knapping experiment was performed using chert from the Western Lessini Plateau (Venetian Prealps, Italy) and belonging to the Maiolica and Scaglia Variegata carbonate formations (Bertola, 2001). Although we did not deliberately aim for specific morphologies or sizes, we selected a sample representative of the raw material variability described in previous petrological analyses and technological investigations at the site of Fumane Cave (Bertola, 2001; Falcucci et al., 2017). A total of eight knapping sequences were carried out using six raw material core blanks, weighing from 220 to 1080 g and with different percentages of cortex coverage. A big-sized nodule was in fact broken into more chunks in the early stages of its reduction and the two largest detached pieces were also used as core blanks for laminar production (see more information in Supporting Information S1).

We digitally recorded the progressive exhaustion of cores using an Artec Space Spider 3D scanner (Artec Inc., Luxembourg) following the

protocol described in Göldner et al. (2022). Each core was scanned and weighted with a digital scale prior to the beginning of the knapping and at different stages of blank production until the core's discard. Depending on the initial size of the core and the progression of the knapping, a minimum of four to a maximum of ten scans were performed, thus digitizing a total of 50 cores. We scanned the cores after each set of blank extraction along the flaking surfaces. Furthermore, we also recorded maintenance operations that resulted in the extraction of a significant portion of the cores' volume, even when this involved the removal of a single large blank. This approach allowed us to have an accurate snapshot of each relevant knapping stage, accounting thus for a significant spectrum of the variability identifiable on an archaeological level and involving complex formation processes linked to site-use strategies (Barton and Riel-Salvatore, 2014). This experimental protocol was also ideal to test the VRM in a diachronic perspective; an aspect of uttermost relevance when dealing with core technologies involving a progressive volume depletion along one major volumetric axis. 3D meshes of these experimental cores can be downloaded in the research compendium to this paper (Lombao et al., 2023a).

2.2. The archaeological dataset and the raw material variability

The archaeological assemblage analyzed in this study comes from the earliest Protoaurignacian units excavated at Fumane Cave in the Venetian Prealps (Fig. 1). This site is a reference sequence for the Middle and early Upper Paleolithic in northeastern Italy and systematic excavations have been carried out since the eighties by the University of Ferrara (Peresani, 2022). Here we consider the Protoaurignacian layers A2 and A1 as a single assemblage, based on several archaeological and chronological lines of evidence (see discussion in Falcucci et al., 2017). The Protoaurignacian in A2–A1 dates to 41.2–40.4 ky cal BP (Benazzi et al.,

2015; Higham et al., 2009) and contains one of the earliest evidence for the replacements of Neanderthals by *Homo sapiens* in Europe (Benazzi et al., 2015). This lithic assemblage has been the object of several techno-typological and functional studies (Aleo et al., 2021; Bertola et al., 2013; Falcucci et al., 2017, 2020; Falcucci and Peresani, 2018).

The core classification used in this study has been proposed by Falcucci and Peresani (2018), who mainly considered the location of the flaking surface and the progression of knapping. This classification primarily differentiates between cores in which the flaking surface is oriented according to the longitudinal axis of the selected blank to obtain elongated and straight products and cores in which the flaking surface is oriented according to the transversal axis of the blank (i.e., carinated cores). The latter are poorly attested compared to Early Aurignacian assemblages described in southwestern France and Central Europe (Bataille and Conard, 2018; Bordes, 2005; Teyssandier, 2007). Cores have been further subdivided according to the scars visible on the flaking surface/s at discard, differentiating between blade, bladelet, and flake scars (Table 1).

All the technological attributes of the A2–A1 assemblage needed to replicate this analysis are derived from Falcucci et al. (2017) and can be found in the associated research compendium (Lombao et al., 2023a). To conduct this analysis, we have 3D-scanned all cores linked to blade and bladelet productions using the same protocol applied to the experimental dataset. These artifacts are now part of an open-access dataset in Zenodo (CC BY 4.0) and can be fully downloaded for scientific and teaching purposes (Falcucci and Peresani, 2023).

The blanks dataset by Falcucci et al. (2017) include blades, bladelets, and flakes bigger than 1.5 cm in maximal dimensions. Besides recording several discrete and metric attributes related to the technological features of the assemblage, artifacts were sorted out into different raw material types following the macroscopic descriptions provided by

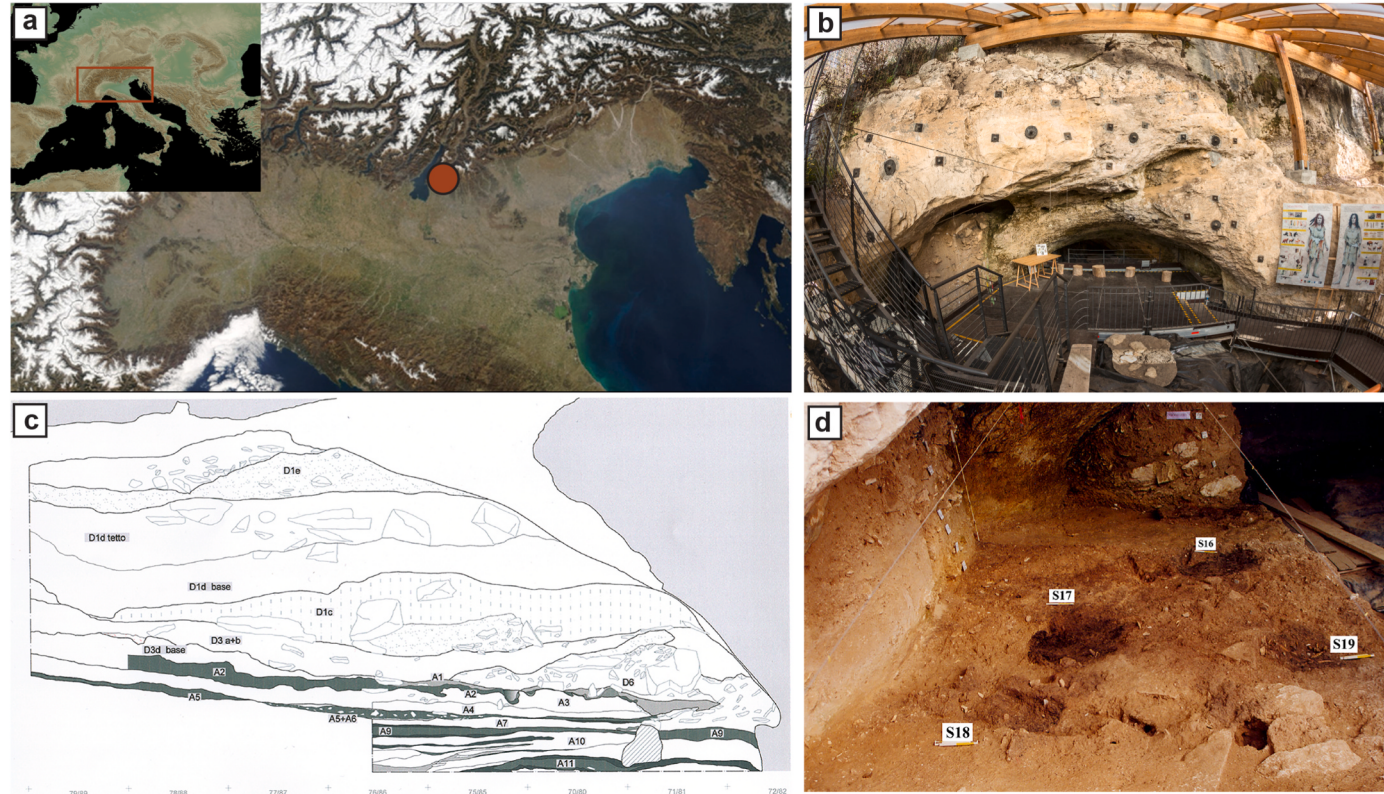


Fig. 1. a) Physical map of Europe showing the geographical location of Fumane Cave (red dot) in northeastern Italy; b) View of the site's main tunnel A, featuring modern scaffolds for musealization purposes; c) Sketch of the cave's transversal section displaying evidence of the late Mousterian (A11–A4), Uluzzian (A3), early Protoaurignacian (A2–A1), late Protoaurignacian (D6–D3a + b), and the stratigraphic complex D1 (section drawn by M. Peresani and S. Muratori); d) Excavation of layer A2 with concentration of anthropogenic features (S16–S19) in the western sector of the cave entrance.

Table 1

Cores from the A2–A1 assemblage recovered at Fumane, categorized by raw material and blank production (percentages are shown in brackets). The “Other” category includes sparsely attested raw material varieties. In the figures below, the term “Scaglia” is abbreviated as “S” (e.g., S_Variegata) for better data visualization.

Raw material	Flake	Blade-Bladelet	Blade-Flake	Bladelet	Total
Maiolica	4 (4.4%)	27 (29.6%)	9 (35.1%)	51 (56%)	91 (73.3%)
Scaglia Rossa	–	–	–	6 (100%)	6 (4.8%)
Scaglia Variegata	2 (22.2%)	1 (11.1%)	1 (11.1%)	5 (55.5%)	9 (7.2%)
Scaglia Variegata type 3	1 (6.2%)	5 (31.2%)	–	10 (62.5%)	16 (12.9%)
Other	–	1 (50%)	–	1 (50%)	2 (1.6%)
Total	7 (5.6%)	34 (27.4%)	10 (8.1%)	73 (58.9%)	124 (100%)

[Bertola \(2001\)](#). Raw materials recovered at Fumane Cave are made in most cases on chert from different carbonate formations found in the western Lessini Plateau spanning from the Upper Jurassic to the middle Eocene. They could all be collected within a range of a few kilometers from the site, both in primary outcrops, in loose stream or fluvial gravels, and on the frequent slope-waste deposits and soils. The most common types could be found within a 5 km crow flies radius from the site and are the so-called Maiolicae, Scaglia Variegata, and Scaglia Rossa. Particularly abundant are the Maiolica and the Scaglia Variegata ([Delpiano et al., 2018](#)). All the used raw materials at Fumane have excellent flaking properties, although the Scaglia Variegata can have different quality and sizes according to the specific sub-type ([Bertola, 2001](#)). In this regard, a very frequent occurrence in the Protoaurignacian is the yellow-gray type (SV3; also known as Pietra Gallina) of the Scaglia Variegata, which is of excellent quality and can be easily sorted from the rest of the sub-types thanks to different macroscopic features. We will thus keep this sub-type separated in the analysis to have a more refined outlook of raw material management strategies in the Protoaurignacian. Other formations, such as the Tertiary sandstones and the Oolitic limestones are rarer, although a few large-sized blades made on Oolitic flint were recovered in the early Protoaurignacian ([Falcucci et al., 2017](#)). In this study, these marginal varieties from a quantitative point of view, were grouped in the category “Other”.

2.3. Reduction intensity proxies

To quantify reduction intensity proxies, all 3D meshes of the cores were analyzed in the open-source software Meshlab ([Cignoni et al., 2008](#)). We quantified volume, surface area, cortical surface area, and linear dimensions (i.e., length, width, and thickness). We preferred to use a technological orientation of the core instead of measuring the main morphological dimensions. Protoaurignacian laminar cores can in fact be effectively oriented in the 3D space considering well-identifiable parameters such as the position of the striking platform and flaking direction; the latter being most of the times unidirectional. To calculate the SDI, we counted all visible scars on the surface of the cores following [Clarkson \(2013\)](#), except for those removals shorter than 5 mm in maximal dimension, as they are likely related to the trimming operations conducted prior to each blank removal. The surface area of each core was measured in Meshlab. Furthermore, we have logarithmically transformed the SDI data, resulting in LogSDI, to assess whether the logarithmic transformation of SDI yields stronger correlations with the actual percentage of extracted volume compared to unmodified SDI. SDI has been applied to all types of cores, irrespective of the type of blank on which they are produced (cores on flakes, etc.).

Finally, we calculated the mean striking angles (i.e., the angle between the platform and the flaking surface) using the Virtual Goniometer plugin ([Yezzi-Woodley et al., 2021](#)) in Meshlab. We took a total of three measurements along the cores’ striking platforms, favoring the areas from which the last sets of successful removals were visible on the flaking surface. The resulting average of the three measurements was used for further analysis.

2.4. Volumetric Reconstruction Method

The main goal of the VRM is to estimate the original volume of cores prior knapping. In this work, we have made a series of changes with respect to the original proposal presented by [Lombao et al. \(2020\)](#) to adapt the methodology to this specific case study. These changes affect both the correction units (i.e., the set of products resulting from the knapping activities) and the association of these units to the maximum dimensions of the cores. Regarding cores, we have standardized the dimension correction system by orienting and measuring core meshes following the maximum technological dimensions at discard. Artifacts are oriented in a way that the length corresponds to the extension of the flaking surface with the striking platform placed at the top (see [Fig. 2](#)). To reconstruct the original dimensions of the unmodified blank, different procedures are applied depending on each technical axis (length, width, thickness). The most significant change to the original application concerns the way in which the length of the cores is calculated. Instead of using a single correction unit for the length, two groups of correction units are established: one for the platform (platform length) and another for the core’s base (distal length). Within the length axis, we refer to platform length as the sector where the striking platform is located, whereas with distal length to the base of the cores (i.e., where the distal part of the blank removals would be located). This was done to account for the frequent use of core tablets (see below) in Upper Paleolithic laminar technologies, which are typically thicker than other flakes detached from blade and bladelet cores ([Inizan et al., 1995](#)). It is important to note that this adaptation has been carried out focusing on the unidirectional Protoaurignacian cores. In the case of bidirectional cores, such as for instance in the early Ahmarian ([Abulafia et al., 2021](#)), a correction unit relative to the platform length should be applied at both extremes of the core. The core’s width and thickness remain unchanged from the original proposal, with a single correction system for both dimensions. As for the correction units, they are calculated following the same procedure as in the original method, which uses the diacritical analysis of the cores to identify the number of generations for each of the discussed technological axes (see [Fig. 2](#)). By generations, we mean the number of scars that overlap on the same axis with similar orientation (see [Lombao et al., 2020](#)). Importantly, for the analysis of experimental cores, we considered only the generations of removals that were visible on the 3D meshes. This approach ensures full alignment between the results of our experimental protocol and the analysis of the archaeological core assemblage, even in those cases where prior known generations were erased by the continuation of stone tool production.

The distinction between platform length and distal length implies an adaptation of the correction units. First, central values of maximum thickness (either mean or median, depending on data distribution) of flakes and tablets from the lithic assemblage associated with the cores are used to correct the platform length. Second, central values of the thickness of flakes, blades, and bladelets are used to correct the distal length, as well as the width and thickness of cores. It is essential to incorporate the thickness of flakes into the correction process for these latter dimensions, as flakes are commonly utilized in the Protoaurignacian at Fumane for initializing blade and bladelet cores, as well as maintaining the flaking surface and core’s flanks throughout the reduction sequence ([Falcucci et al., 2017](#); [Falcucci and Peresani, 2018](#)).

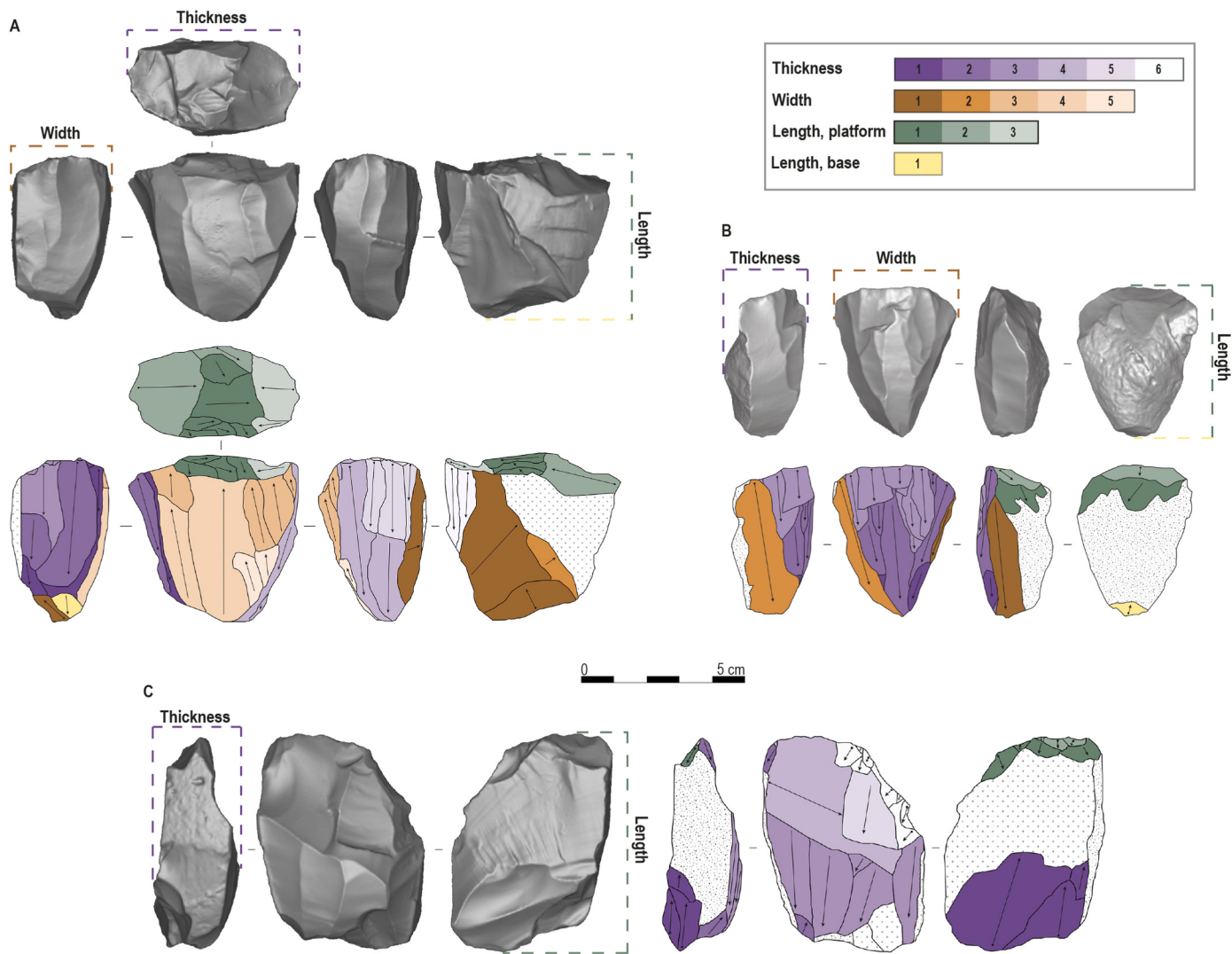


Fig. 2. Application of the revised version of the Volumetric Reconstruction Method to three Protoaurignacian cores from Fumane Cave. Each core is presented as a 3D model, showcasing various views and color-coded drawings. The legend provides an explanation of the numbers and colors, where darker shades represent the oldest phases, indicating the generations for each technological axis, including thickness, width, platform length, and base length. For thickness and width, it is needed to sum the generations from both opposite surfaces affecting these dimensions. Dotted lines surrounding the 3D views of the cores indicate the dimensions influenced by the computed generations, which are counted using a diacritic approach. This approach involves identifying a set of non-overlapping removals associated with a specific reduction phase. In some cases, a generation may correspond to only a single visible removal. A detailed description accompanies each of the displayed cores, offering comprehensive information about the number of generations identified: A) This multiplatform core exhibits multiple visible generations, counted after positioning the core according to the final phase of blank production. It shows five generations for thickness, five for width, three for platform length, and one for base length. B) This semi-circumferential core displays three generations for thickness, two for width, two for platform length, and one for base length. C) This wide-faced core exhibits six generations for thickness and two for platform length. The width does not appear to have been modified by removals. (For interpretation of the references to color in this figure legend, the reader is referred to the Web version of this article).

To do so, we measured the maximum thickness of all experimental and archaeological products bigger than 15 mm in maximal dimension. Additionally, a novelty in this VRM adaptation is the exclusive use of central values of the thickness of products as correction units, instead of platform thickness. This is mostly because Protoaurignacian knappers used marginal percussion to detach blades and bladelets, which often display punctiform or linear platforms (Falcucci et al., 2017). These measurements would arguably not reflect the thickness of the extracted products. Once the number of generations of removals is identified for each technical axis on the core, the number of correction units is multiplied by the central values obtained from the set of flakes, blades, and bladelets for distal length, width, and thickness. For platform length, central values obtained from the assemblage of flakes and core tablets are employed.

Subsequently, the obtained values are added to the core dimensions.

In the case of length, the values obtained for platform length and distal length are both added. For width and thickness, the same procedure as in the original proposal is followed, and the corresponding geometric formula (i.e., ellipsoid, cylinder, sphere) is applied using the corrected dimensions to obtain the estimated original volume (EOV). By dividing the volume of the core by the estimated original volume of the blank prior to knapping, and multiplying the result by 100, we obtain the percentage of the remaining volume on the core. Finally, by subtracting the percentage of the remaining volume from 100, we can calculate the percentage of the extracted volume (PEV) for each of the analyzed cores.

As in previous studies (Cueva-Temprana et al., 2022; Lombao et al., 2020, 2023c), we excluded cores on flake from the VRM analysis. This type of core likely requires additional and/or significant modifications to the original version of the VRM and further experimental activities.

2.5. Statistical analysis

2.5.1. Experimental data

To evaluate the performance of the VRM adaptation, the EOV and the PEV were calculated using different geometric formulas, namely the cube, prism, sphere, cylinder, and ellipsoid. Descriptive statistical analysis was conducted on the Original Volume (OV) of nodules before knapping and the percentage of Extracted Volume (PEV). This analysis included measuring central values such as mean and median, data dispersion values such as maximal and minimal values, standard deviation, coefficient of variation, and normality of the distribution through multiple Shapiro-Wilk tests. We performed all analyses both on real experimental data and the estimates obtained from the application of different geometric formulas. Subsequently, we applied Average Error (AE), Mean Absolute Error (MAE), and Root Square Mean Error (RSME) to evaluate the accuracy of the estimations obtained through the different geometric formulas with respect to the actual reduction data.

The AE – also known as mean error – is a measure of accuracy that shows the difference between the actual and predicted values. To compute this measure, it is necessary to calculate the difference between each predicted value regarding the actual value, and then calculate the mean of these differences. A positive AE means that the predicted values are, on average, higher than the actual values. On the opposite side, negative AE means that the estimations are lower than the actual values. The magnitude of the average error indicates the overall level of accuracy of the predictions or estimations, with a smaller magnitude indicating greater accuracy.

The MAE measures the average absolute difference between the predicted and the actual values in a dataset. As in the case of the AE, it is first necessary to obtain the difference between each predicted value compared to the actual one. However, given that the negative values are transformed into positive ones, it gives the magnitude of the error without considering its direction (i.e., positive, or negative). Next, it is necessary to calculate the mean of the absolute errors. The closer the MAE gets to 0 values, the more accurate the estimations will be. The RMSE is calculated by taking the square root of the average of the squared differences between the predicted values and the actual values. It is worth noting that the RMSE is sensitive to outliers, so it can be a good tool for detecting extreme values.

Using the average of the real data as a reference, it is possible to obtain the percentage of Average Error (%AE), the percentage of Mean Absolute Error (%MAE), and the percentage of the Root Mean Squared Error (%RMSE), which will allow us to directly compare the accuracy of the different geometric volume formulas tested. Additionally, we used the Bland-Altman test (Bland and Altman, 1995) to evaluate the agreement between the two different measurement methods. This test involves plotting the differences between the measurements of the two methods and the average of the measurements on a scatter plot. The plot also includes the mean line of the differences and the agreement limits. The mean line represents the average difference between the two measurement methods, while the agreement limits represent the expected range of agreement between the two measurements. Finally, we compared the correlations between real values for percentage of extracted volume and the estimated percentage of extracted volume for each core or reduction sequence.

After evaluating the adaptation of the VRM, we proceeded to analyze the correlations between different reduction intensity methods (e.g., VRM, SDI, percentage of non-cortical surface, angle, etc.) with respect to the actual percentage of extracted volume during the experiment. As some variables had a non-normal distribution according to a Shapiro-Wilk test ($p < 0.05$), both Pearson's r and Spearman's Rho were used, following previous applications (Lombao et al., 2020).

2.5.2. Archaeological data

We performed the descriptive statistics to the core assemblage from Fumane Cave using the procedures already described for the

experimental material. We then conducted a Weibull distribution analysis (Dorner, 1999; Pasha et al., 2006; Shott, 2002) to examine differences in raw material reduction intensity. The Weibull distribution analysis is commonly employed to model and analyze failure or survival time data. In lithic studies, it is frequently utilized to describe the discard rate of a product or system over time or reduction intensity. The Weibull distribution comprises two parameters (i.e., shape and scale), which determine distribution and location of the distribution on the time (i.e., reduction intensity) axis. The shape parameter can be less than, equal to, or greater than 1, corresponding to a failure distribution that is decreasing, constant, or increasing over time or reduction, respectively. The Weibull distributions were calculated with maximum likelihood estimation method using the “fitdist” function provided by the R-package *fitdistrplus* (v.1.1-8) (Delignette-Muller and Dutang, 2015).

Furthermore, we conducted non-parametric Kruskal-Wallis (K-W) tests to identify any significant differences between the medians of two or more independent groups, such as raw materials, core types, or types of blank production. When necessary, we applied post-hoc Dunn tests to determine which pairs of groups differ significantly from each other. Finally, we utilized the Kolmogorov-Smirnov (KS) test to compare distributions.

All methodological procedures for calculating both the original volumes and the percentage of Extracted Volume through VRM using different geometric formulas, as well as all statistical steps carried out in this study, were performed in R (4.2.2v) within the R Studio environment (Posit team, 2023; R Core Team, 2022), using different packages for statistical analysis and visualization (i.e., Delignette-Muller and Dutang, 2015; Wickham, 2016, 2011, 2007; Wickham et al., 2023). The R Markdown and datasets required to reproduce this work are available on Zenodo (CC BY 4.0 license) (Lombao et al., 2023a).

3. Results

3.1. Testing the adaptation of the Volumetric Reconstruction Method

The estimated volumes obtained using the prism and cube geometric formulas exhibit central mean and median values that are considerably higher than the real data, sometimes doubling or even tripling the original volumes (see Fig. 3). However, the other considered geometric shapes, including the cylinder, ellipsoid, and sphere, have slightly lower medians than the actual volumes (see Table 2).

Regarding the data dispersion, we observe that the estimated volumes obtained from the geometric formulas show a higher Coefficient of Variation (CV) compared to the experimental data. This discrepancy can be explained by the sequential nature of the experiment, in which all the cores originated from eight distinct blanks, resulting in the original volumes being concentrated in eight specific values, whereas reconstructions always end up generating different values and therefore more variability.

While there are statistically significant differences between the different central values of both the actual and estimated volumes (K-W; $H = 30.871$, $df = 5$, $p < 0.05$), further post-hoc analysis indicates that these differences are exclusively between the estimated volumes obtained using the cube formula and the estimations obtained using the sphere and ellipsoid formulas (see Supplementary Table S1). This suggests that the estimated volumes have central values that are similar to the actual data.

To assess the accuracy of each geometric formula, we calculated the AE, MAE, and RMSE for each class. We found that the estimated volumes obtained through the cylinder formula have the lowest error in terms of both the original volume, as determined by AE and %AE. However, since positive and negative errors can cancel each other out in this test, we also evaluated the direction of the errors using MAE. In this test, the ellipsoid and cylinder produced the lowest results. Finally, we calculated the RMSE, which is the square root of the average of the squared differences between the predicted and actual observations. This test

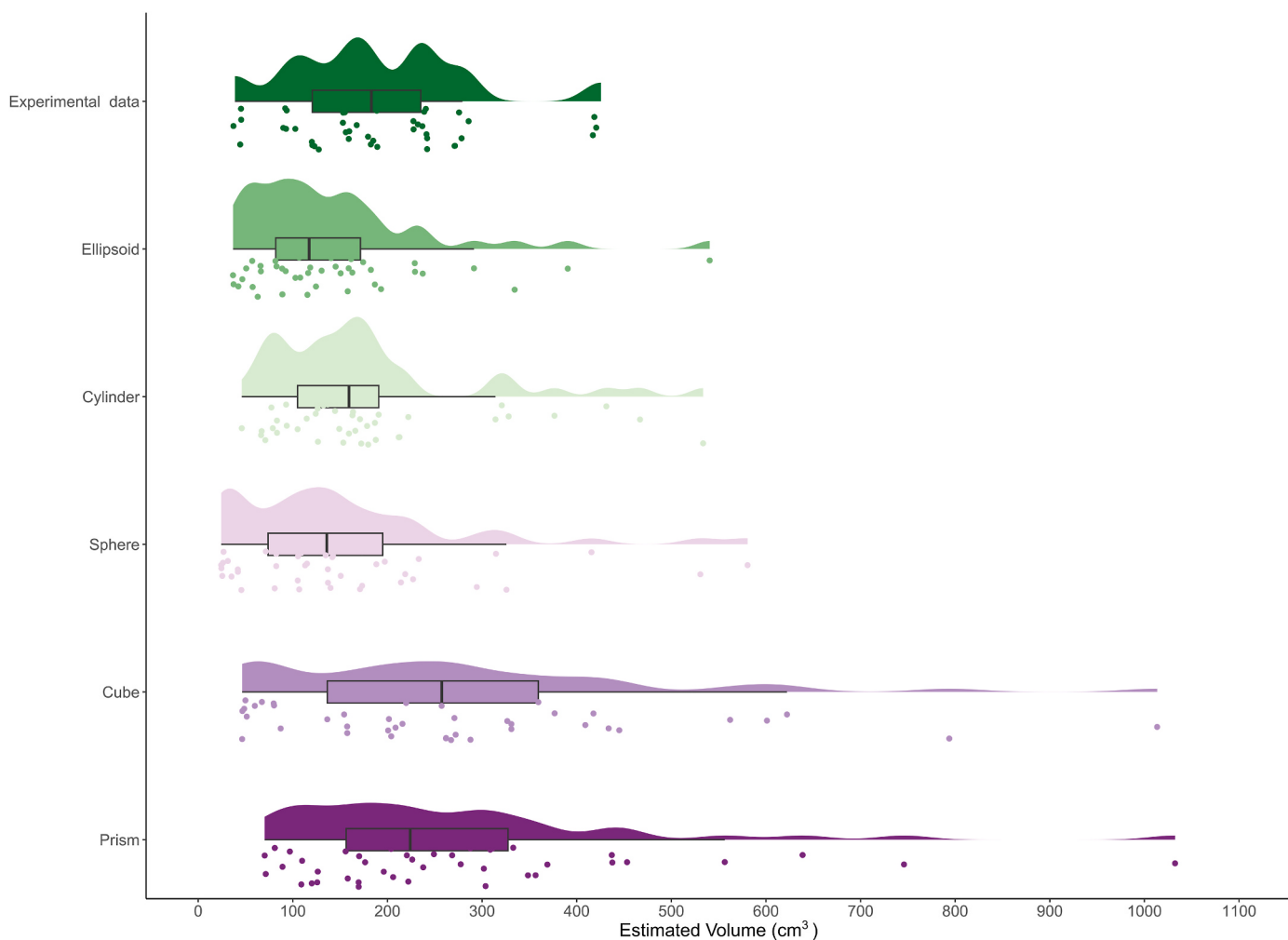


Fig. 3. Boxplots with jittered points and histograms showing a comparison of the estimated original volumes (EOV; cm^3) obtained from different geometric formulas.

Table 2

Descriptive statistics for Estimated Volumes (in cm^3). N = sample size. Min = minimum value, Max = maximum value, SD = Standard Deviation, CV = Coefficient of Variation, S-W = Shapiro-Wilk test, Exp. Data = Experimental data.

Geometries	N	Mean	Median	Min	Max	SD	CV	S-W
Exp. Data	42	189.41	183.01	38.77	425.62	96.91	0.51	0.01
Prism	42	274.49	224.12	70.20	1032.43	193.02	0.70	<0.001
Cube	42	297.24	259.64	46.46	1109.04	245.15	0.82	<0.001
Sphere	42	155.63	135.95	24.33	580.69	128.36	0.82	<0.001
Cylinder	42	208.41	161.17	46.02	1343.43	211.27	1.01	<0.001
Ellipsoid	42	143.72	117.35	36.76	540.58	101.07	0.70	<0.001

Table 3

Results of Average Error (AE), Mean Absolute Error (MAE), Root Mean Squared Error (RMSE), and their percentages (%) for each geometric formula used.

Geometries	AE	%AE	MAE	%MAE	RMSE	%RMSE
Prism	85.08	44.92	120.43	63.58	173.61	91.66
Cube	107.83	56.93	169.95	89.72	244.23	128.95
Sphere	-33.78	-17.83	96.06	50.72	126.56	66.82
Cylinder	19.00	10.03	83.72	44.20	168.40	88.91
Ellipsoid	-45.69	-24.12	68.27	36.04	96.82	51.12

penalizes larger errors more heavily. In this sense, the ellipsoid presents slightly better results, since its RMSE and %RMSE are lower (Table 3). In fact, in the error distribution (Fig. 4) the ellipsoid has a smaller error

range, although the distribution itself indicates that in some cases there is a severe underestimation of the original volume.

These oscillations in the original estimated volumes logically affect the estimated percentages of extracted volume depending on whether there is a general tendency to overestimate or underestimate the original volume values. Thus, those original volumes that are overestimated tend to have higher average extracted volume percentages (i.e., cube and prism), being more similar to the estimated extracted volume percentage values through the ellipsoid and cylinder volume formulas (Table 4).

Again, the result of the K-W analysis shows statistically significant differences between the extracted volume percentages ($H = 54.036$, $df = 5$, $p < 0.05$). Further analysis (Dunn test) indicates that these differences are between the estimates obtained from different geometric

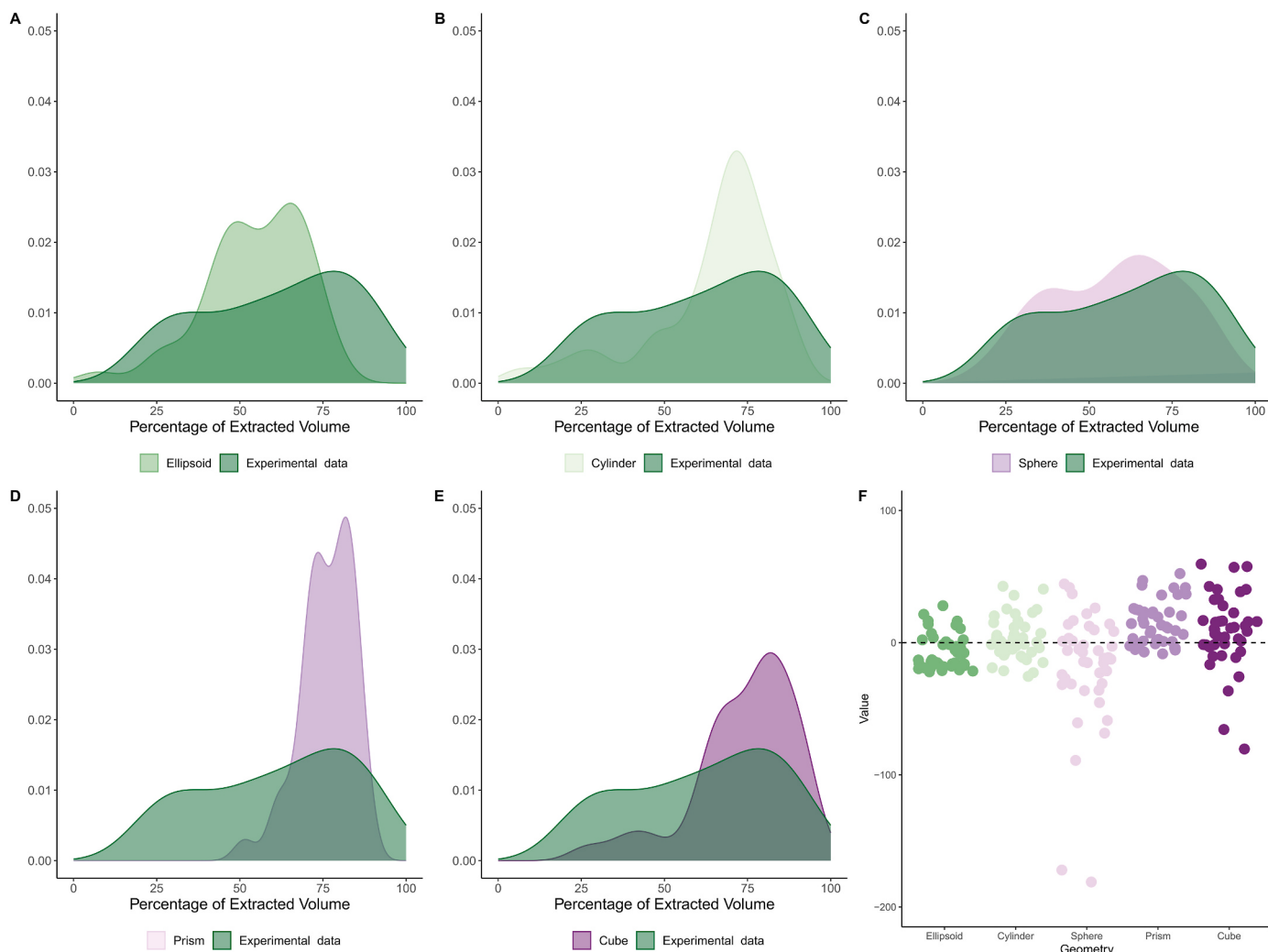


Fig. 4. A-E) Comparisons of Percentage of Extracted Volume distributions between each geometric formula and real data. F) Jitter plot illustrating individual errors, which represent the differences between individual real data points and its estimation based on each geometric formula. Negative values (below 0% of extracted volume) were excluded in graphs C (sphere) and E (cube), as they represent unrealistic values, but are included in graph F.

Table 4

Descriptive statistics for the Percentage of Extracted Volume (PEV). Values are reported in percentages. N = sample size. Min = minimum value, Max = maximum value, SD = Standard Deviation, CV = Coefficient of Variation, S-W = Shapiro-Wilk test.

Geometries	N	Mean	Median	Min	Max	SD	CV
Exp. Data	61.25	65.26	21.05	95.11	22.44	0.37	0.02
Prism	76.18	76.99	51.43	87.80	7.90	0.10	0.02
Cube	69.80	76.99	-16.90	93.61	24.20	0.35	<0.01
Sphere	42.33	56.06	-123.26	87.80	46.22	1.09	<0.01
Cylinder	64.41	70.27	6.05	87.78	19.23	0.30	<0.01
Ellipsoid	54.51	56.06	7.24	76.69	15.10	0.28	0.02

formulas, without finding significant differences between the actual values and the different estimates (Supplementary Table S2).

It is possible to observe a certain disparity in the distributions obtained between the different formulas, which indicates an unequal performance when estimating the core reduction intensity. The K-S test shows us that in fact, apart from the cylinder and the sphere, the rest of the geometric formulas present statistically significant differences in the distribution. Moreover, in the case of the sphere, although it does not present statistically significant differences, the errors between individual observations show how in some cases the geometric formula is not adequate to reconstruct the original size of the nodule, obtaining

individual errors in extreme cases of almost -200% (Fig. 4F).

Again, the AE, MAE and RMSE values, as well as their respective percentage values, indicate a better performance of the cylinder and ellipsoid compared to the other geometric formulas. In fact, on average, these errors generally account for less than 15% of the extracted volume in the three indexes, indicating an optimal efficiency of these geometric formulas in estimating the degree of reduction intensity (Table 5). Also, the correlations between the percentage of extracted volume and the percentage of extracted volume estimated by each of the geometric formulas indicate a strong and positive correlation for the ellipsoid ($r = 0.81$, $r^2 = 0.65$ $p < 0.001$) and the cylinder ($r = 0.70$, $r^2 = 0.48$ $p < 0.001$), confirming their effectiveness as reduction intensity indexes.

Table 5

Results of Average Error (AE), Mean Absolute Error (MAE), Root Mean Squared Error (RMSE), and their percentages (%) for each geometric formula used.

Geometries	AE	%AE	MAE	%MAE	RMSE	%RMSE
Prism	14.94	24.38	16.80	27.44	22.22	36.27
Cube	8.56	13.97	21.52	35.14	29.22	47.71
Sphere	-18.92	-30.89	30.93	50.50	48.94	79.91
Cylinder	3.17	5.17	12.19	19.90	16.39	26.76
Ellipsoid	-6.73	-11.00	13.20	21.54	14.86	24.26

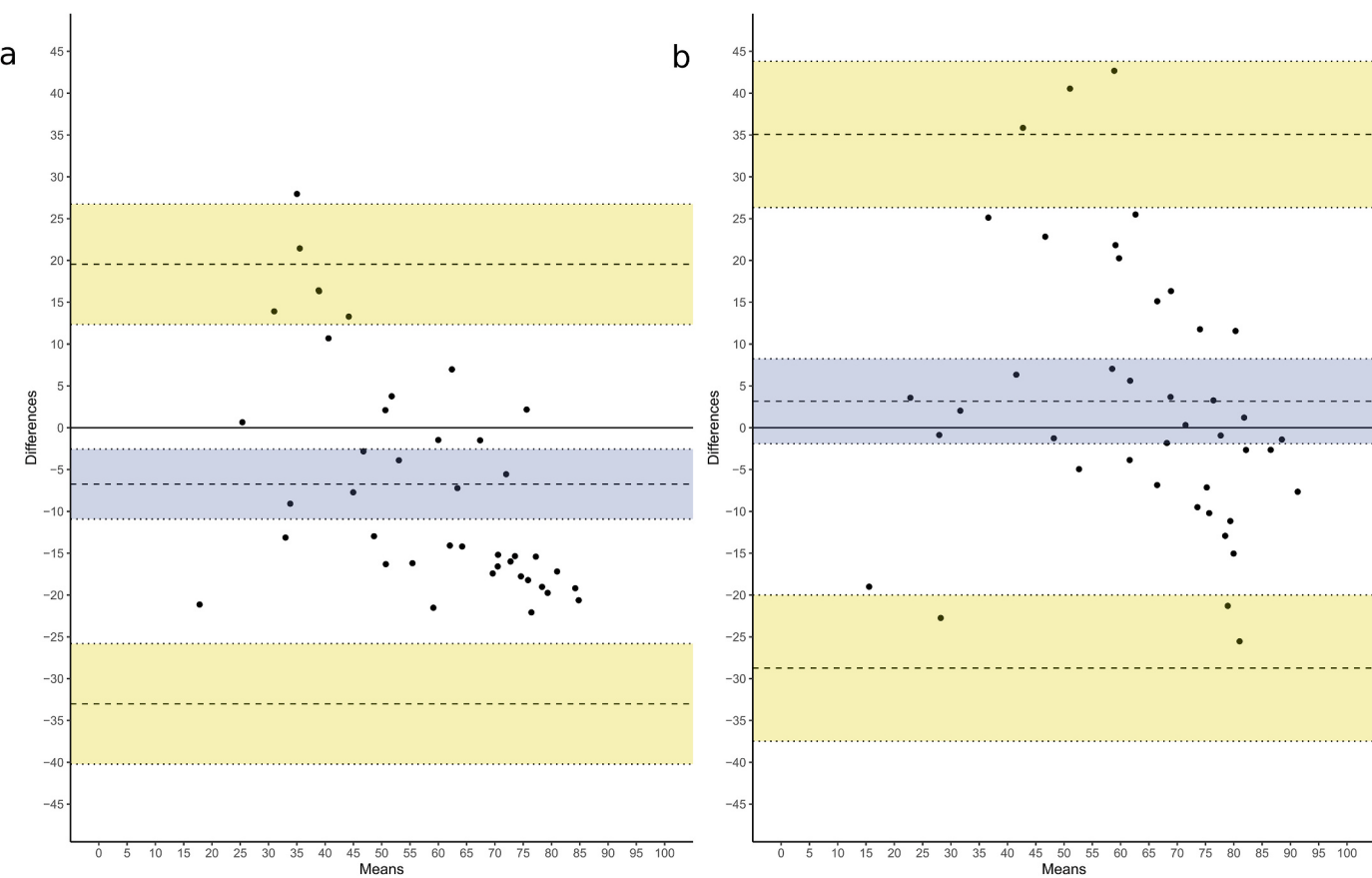


Fig. 5. Visualization of the Bland-Altman test for the a) ellipsoid, and b) the cylinder formulas.

To elucidate which of the geometric formulas is more accurate between the ellipsoid and the cylinder, we performed a Bland-Altman analysis, a graphical method for comparing two measurement techniques on the same quantitative variable. Thus, for the ellipsoid (Fig. 5a), there is a bias of -6.73 , a lower limit of agreement of -33.01 , and an upper limit of agreement of 19.54 . Although this range of agreement includes the value 0 , which is indicative of good performance, the bias is significant since the 95% confidence interval of the bias (from -2.55 to -10.91 ; blue region around the central dashed line) does not include the value 0 . The distribution of the individual errors also shows a tendency to overestimate reduction intensity in the first phases of reduction sequences (between 25 and 40% of extracted volume) and infra-estimate reduction intensity in the last phases (from 50% to 90%).

Instead, for the cylinder (Fig. 5b), there is a bias of 3.16 , a lower limit of agreement of -28.73 , and an upper limit of agreement of 35.06 . This range of agreement is wider than in the case of ellipsoid but also includes the value 0 . Further, the bias is not significant since the 95% confidence interval of the bias (from -1.01 to 8.23) includes the value 0 which means a concordance between the real and estimated values through the cylinder volume formula. Lastly, regarding the cases with larger differences, it is important to consider that they are spread along the X-axis, meaning that larger differences are not correlated by reduction intensity. Furthermore, when analyzing the results within three volume extraction ranges (0 – 30% , 30 – 60% , and 60 – 100%) we observed that the cylinder formula overestimates by approximately 10% on average ($AE = 8.94$) in the 0 – 30% range. This overestimation increases to 12.9% in the 30 – 60% range, but results in a slight underestimation in the more advanced reduction phases (60 – 100%) with an AE of -4.02% (see Supplementary Table S5, Supplementary Fig. S1).

Despite the tendency to overestimate in the early stages and slightly underestimate in the later stages of reduction sequences, our comparison

of correlations between actual values for the percentage of extracted volume and the estimated percentage obtained through the cylinder for each individual core or reduction sequence reveals consistent findings (see Supplementary Fig. S2). Our results indicate a consistently high, positive, and statistically significant correlation between these values for each core throughout the reduction sequence, with correlation coefficients ranging from $r = 0.88$ to $r = 0.99$. However, in three cases, this correlation is not statistically significant ($p > 0.05$) due to the small sample size. Having evaluated the advantages and limits of this adaptation of VRM to blades and bladelets cores, we compared the effectiveness of this method with others such as the SDI (Clarkson, 2013), percentage of non-cortical surface, and other technical attributes such as the angle between the striking platform and flaking surface, the number of striking platforms, the number of exploited surfaces, the number of convergences between exploitation surfaces (following Douglass et al., 2018), and finally the number of rotations to observe which of these variables may be correlated and be a good reduction proxy (Table 6).

The results indicate a strong and positive correlation between the percentage of extracted volume and SDI, Log SDI, and percentage of non-cortical surface area (Table 6). Therefore, they will be used in the archaeological study as a complementary control method to the VRM. On the other hand, most of the other variables used (e.g., number of surfaces, number of rotations, and number of platforms) have very low correlation values with respect to reduction and have therefore not been further considered.

Finally, one significant concern when dealing with this type of cores is the potential issue of overlapping effect, in which the new removals eliminate the scars of previous removals on the surface of the cores, as discussed in Lombao and colleagues, (2019). To assess the influence of this overlapping effect, we conducted two sets of analyses for each of the analyzed cores. First, we examined the correlation between the number of scars and each phase. Second, we explored the correlation between

Table 6

Correlation tests comparing percentage of remaining volume and the different attributes considered in this study.

Attributes	Pearson R	Coefficient of determination	P value	Spearman rho	P value
Number of scars	0.51	0.24	<0.001	0.50	<0.001
SDI	-0.70	0.49	<0.001	-0.76	<0.001
Log SDI	-0.78	0.60	<0.001	-0.76	<0.001
Percentage of non-cortical surface	0.78	0.62	<0.001	0.84	<0.001
Number of convergences	-0.42	0.18	<0.001	-0.46	0.001
Number of flaking surfaces	-0.48	0.23	0.001	-0.48	0.001
Number of flaking rotations	-0.08	0.007	0.5	-0.07	0.6
Number of platform surfaces	0.22	0.04	0.1	0.21	0.1
Angle	0.15	0.02	0.3	0.13	0.3

the number of identified generations and each phase. The results consistently reveal strong, positive correlations between these variables, suggesting that, in general, the overlapping phenomenon does not have a significant impact as initially anticipated. However, it is important to note that there are occasional fluctuations in both the number of scars and the number of generations across phases and cores, which may introduce some degree of error in the results. These fluctuations should be considered when evaluating the outcomes of reduction intensity studies on laminar cores (see [Supplementary Figs. S3 and S4](#)).

3.2. Application to the case-study of Fumane Cave

3.2.1. Raw material

The results indicate that there is considerable variation in the

estimated original volumes, ranging from 19 cm³ to 473 cm³. These estimated volumes are similar to the original volumes we employed in the experiment, which ranged between 38.77 cm³ and 425.62 cm³. The raw material varieties used belong in fact to the same source areas described in the archaeological record.

However, there are notable differences in the estimated volumes when results are sorted by raw material type. Maiolica and the Other groups have significantly higher central values than Scaglia Rossa, Scaglia Variegata, and Scaglia Variegata type 3 ($K-W = 10.214$, $df = 4$, $p = 0.037$). These discrepancies can be attributed to the blank used and the inherent properties of each chert type ([Bertola, 2001](#)). The Chi-squared test shows a significant association between the blank types and raw materials ($\chi^2 = 29.33$, $p = 0.02$). Maiolica, for example, had a greater variety of core blanks, including

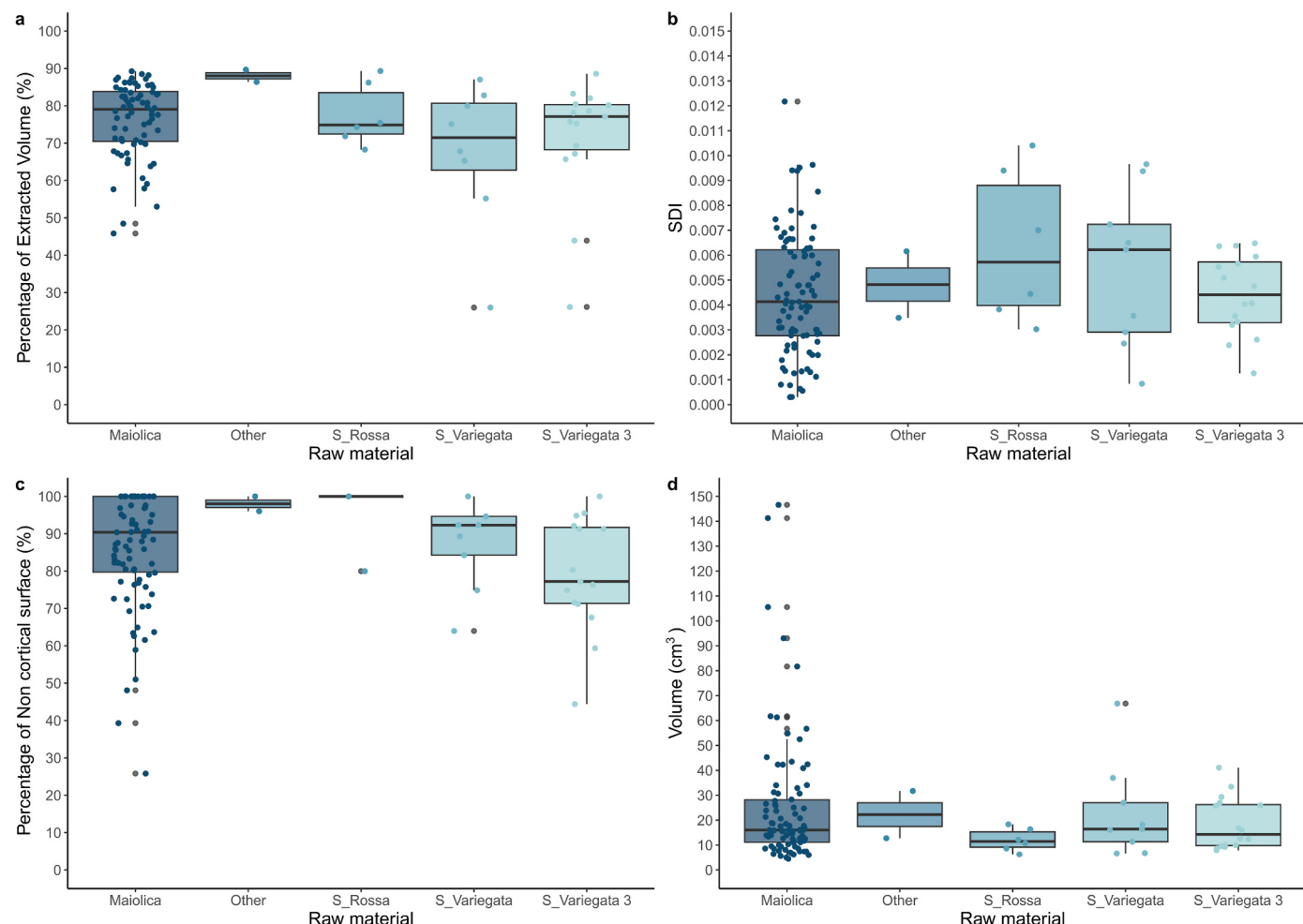


Fig. 6. Boxplots with jittered points showing the results for a) PEV obtained through VRM, b) SDI) c) Percentage of non-cortical surface, and d) volume of the cores according to raw material type.

cores-on-nodules and cores-on-flakes, but also several blanks that could not be identified (i.e., undetermined). Scaglia Variegata, on the other hand, was more commonly found in blocks, whereas Scaglia Variegata type 3 was frequently linked to slabs (Supplementary Table S3).

Notwithstanding these differences in sizes and type of core blanks across raw materials, the reduction intensity estimated using the VRM is relatively high, with central values close to 70–80% of the extracted volume, as shown in Table 7. This trend of high reduction intensity is consistent across the different types of raw materials, as illustrated in Fig. 6 and by the comparable central values across the studied sample (Kruskal-Wallis H = 7.0878, df = 4, p = 0.13). Nevertheless, the cores made from the Maiolica, which is the most abundant at the site, exhibit a higher concentration of lower values in comparison to other chert types. However, Scaglia Variegata and Scaglia Variegata type 3 show more extreme values, leading to a higher variability in the reduction intensity of the cores, as shown by the higher values of the CV for these raw materials. The results of the SDI and the percentage of non-cortical Surfaces (where cores-on-flake are included in the analysis) do support these findings, with the Maiolica cores displaying a higher number of lower values in both proxies (see Table 7).

We conducted a Weibull distribution analysis using the data derived from the VRM to further explore the core reduction patterns across raw materials. We calculated the shape and scale for each raw material, reflecting the degree of variability in the data and the rate of core discard parameters. The results revealed that the Maiolica exhibits the highest shape value, an indication of a relatively consistent and uniform reduction pattern. In contrast, the rest of the raw materials display lower shape values, suggesting greater variability in their reduction patterns. Furthermore, the scale parameter is higher for the Scaglia Rossa,

followed by Maiolica and Scaglia Variegata type 3.

Despite the differences in scale and shape values, the Weibull distributions reveal minimal disparities in the discard patterns of cores across raw materials. In general, the curves tend to be of type I (*sensu* Shott, 2002; Shott and Sillitoe, 2004). Type I curves characterize increasing discard rates with increasing use, a pattern related to attrition in engineering and aging in demographics. So, in general there is a high degree of discard rate when cores are more reduced and exhausted (Fig. 7).

Regardless of the overall trend of high core reduction across all raw materials and the discard of cores at advanced stages of the reduction sequence, subtle differences suggest varying management strategies in relation to raw material types. For instance, the remaining volume of cores indicates that they are generally discarded when volumetrically exhausted. This pattern differs for several cores made on Maiolica, which exhibit a less intensive exhaustion degree. If this finding is compared to other aggregate data, such as the products-to-cores ratio, we observe that Scaglia Variegata type 3 (29.25) and Maiolica (51.38) have lower ratios than the Scaglia Rossa (66.16) and Scaglia Variegata (69), indicating evident differences in the productivity of raw materials (Supplementary Table S4).

3.2.2. Core classification

The category that was classified as being in the early stages of reduction (i.e., initial cores) generally exhibits a lower reduction intensity than other core types. This seems to be logical since initial cores were classified based on various morpho-metric and technological parameters, including the percentage of cortex coverage, the presence of removals related to the shaping of cores' convexities (e.g., core

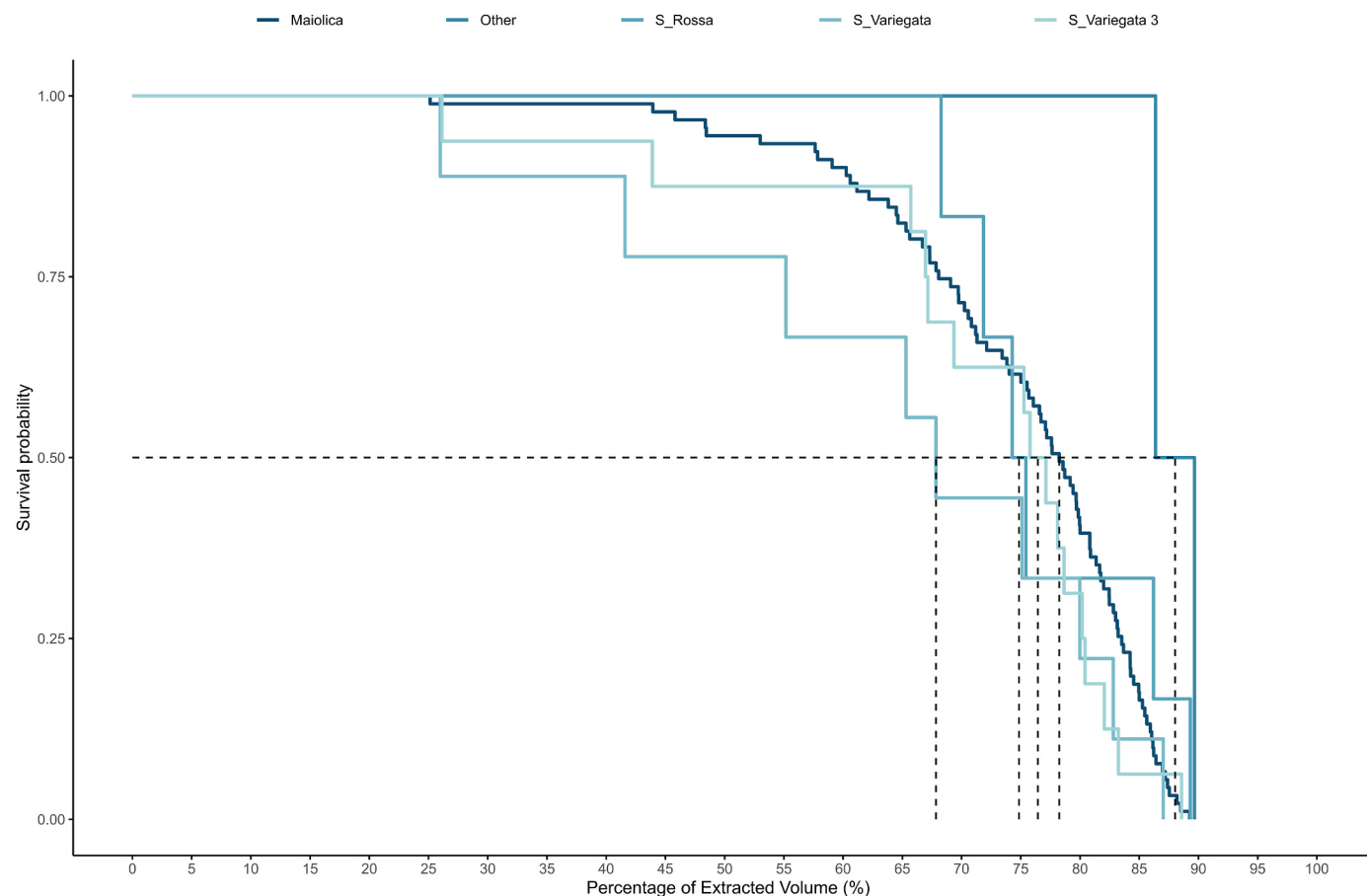


Fig. 7. Kaplan Meier plot showing the survival probability of cores from Fumane Cave by raw material along the reduction continuum (i.e., Percentage of Extracted Volume), as predicted by the VRM.

cresting), and the extent of the flaking surface (see Falcucci and Pernani, 2018). It must be noted, however, that the reduction percentages of initial cores can reach values of up to 70–90% of the estimated extracted volume. Although the VRM shows a tendency to overestimate the reduction intensity of initial cores (around 10%; see 3.1) this finding suggests that core reduction is not a straightforward linear process across phases. Our data highlights instead how core reduction involves a rapid decrease in blank volume during the very initial stages of the reduction sequence. Processes such as core decortication, preparation of a plain and acute striking platform, and the volumetric configuration of both longitudinal and transversal convexities are highly demanding in terms of raw material.

In general, all core types except for initial cores present very low and similar volumes to each other, with no statistically significant differences between them (Kruskal-Wallis $H = 18.58$, $df = 5$, $p = 0.002$), indicating a high level of volumetric depletion regardless the variability of cores (Fig. 8d). Narrow-side cores exhibit a slightly lower degree of reduction intensity compared to other core types. This could be because exploitation focuses on a specific sector of the cores, as the name suggests. In some cases, the abrupt separation between the flaking surface and the cores' flanks was used to extract naturally backed and neo-crested blades to efficiently maintain the transversal convexities. On the contrary, cores classified as wide-faced generally have higher values of estimated percentage of extracted volume and SDI compared to the previous category. This is true for those cores oriented toward the production of both blades and bladelets as well as for cores with both blade

and bladelet negatives visible and cores with only bladelets. Semicircumferential cores show some discrepancies in the reduction intensity if different methods are contrasted. When considering the SDI, semicircumferential cores present higher values compared to both wide-faced and narrow-sided. On the other hand, the values obtained from the VRM are more similar to narrow-sided cores, but lower than wide-faced cores.

Moreover, if semicircumferential cores are sorted according to the production target visible at discard, we can observe that with the VRM there is a similar pattern between the blade-bladelets cores and those oriented exclusively to bladelets. They appear to be at an intermediate point between the narrow-sided and the wide-faced ones. In contrast, the SDI shows a contrasting pattern, characterized by comparable reduction patterns between semicircumferential, narrow-sided, and wide-faced cores. On the other hand, however, bladelet cores show a much higher reduction intensity. These marked discrepancies can be explained by the characteristics of the reduction methods themselves, especially since the SDI also includes cores made on flakes. This could indicate differential management strategies that are to be put in relation to the objective of blank production (see discussion).

Carinated cores exhibit higher reduction intensities, although this core type is mostly related to the use of thick flakes as core blanks. Carinated cores are generally oriented towards the production of bladelets and are reduced along the transversal axis of the blank (Le Brun-Ricalens, 2005). While flaking surfaces are shorter compared to the rest of the core types (Falcucci et al., 2017), bladelet production is

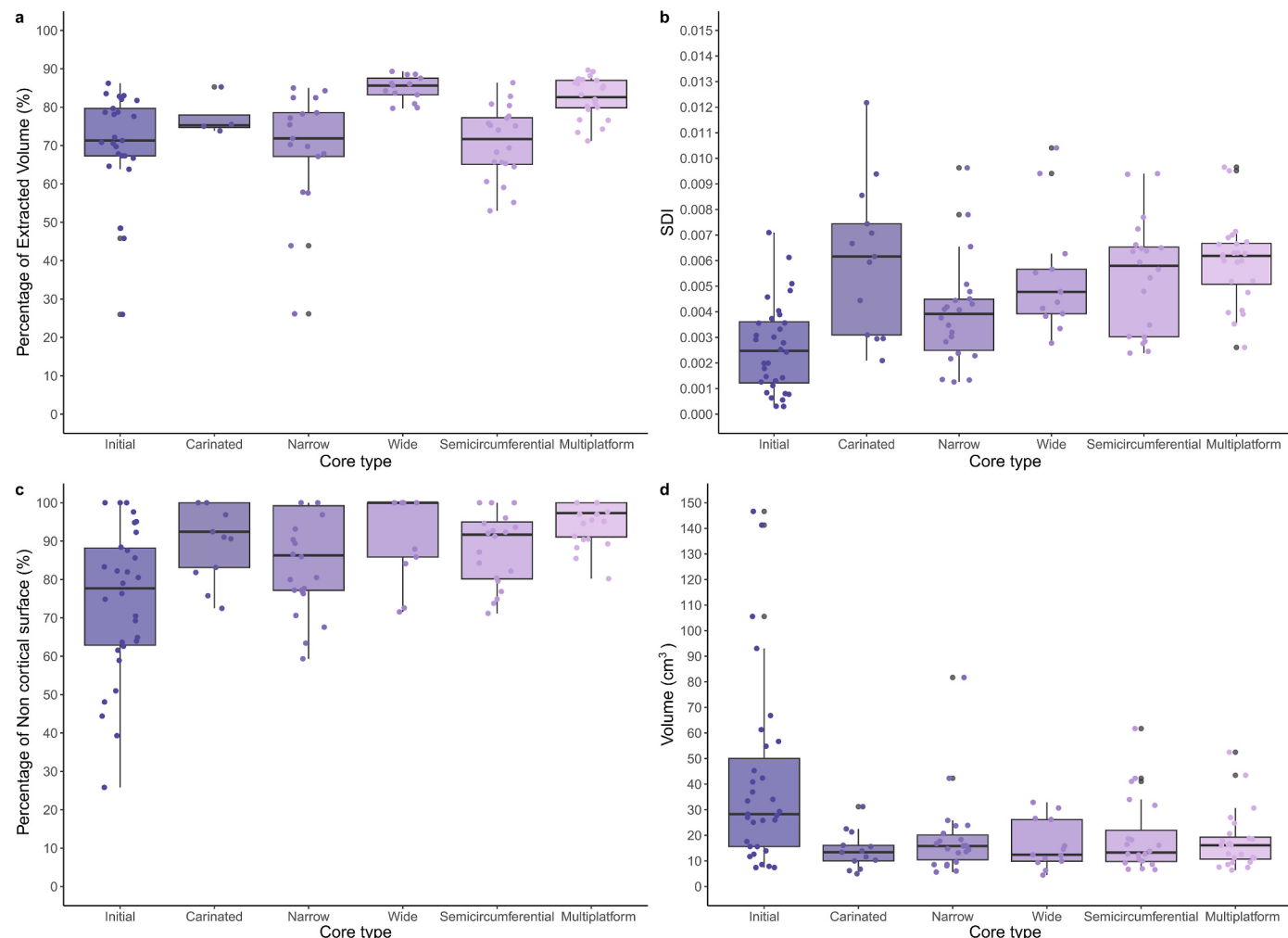


Fig. 8. Boxplots with jittered points showing the results for a) PEV obtained through VRM, b) SDI) c) Percentage of non-cortical surface, and d) volume of the cores according to raw core type.

ideally more effective since cores require little maintenance of the longitudinal convexities and the progression along the longest axis allows for the use of a significant portion of the available volume.

Finally, the higher volumetric depletion and reduction intensity of multiplatform cores indicate that the combination of different reduction procedures is highly effective in maximizing blank production by utilizing most of the available volume.

3.2.3. Blank production

We noticed some discrepancies in the reduction intensity methods when production targets are compared, especially with respect to results from bladelet cores. In these cores, the SDI points to more pronounced differences between blade and bladelet cores, which may be related to the high negative correlations found between size (i.e., volume) and SDI ($R = -0.58$, $p < 0.05$). On the other hand, both the percentage of non-cortical surface and the PEV obtained through VRM suggest no major differences, especially between cores with bladelet and blade and bladelet scars (Fig. 9). Cores with blade and flake scars are generally less reduced, in line with the interpretation of several flake scars as being

related to initialization and maintenance operations carried out in the early stages of reduction (see Falcucci and Peresani, 2018). In this framework, it might be an indication of the presence of cores in which a shift occurs from one target to another (e.g., from blades to bladelets), while others are oriented from the beginning to the production of bladelets.

4. Discussion

4.1. Methodological remarks

In this work, we adapted the VRM method to analyze blade and bladelet cores. To do so, we modified the way in which corrections of technological dimensions are calculated in Lombao et al. (2020) by applying two correction factors to the length axis (i.e., one for the base and another for the striking platform). While this adaptation can slightly slow down the analytical process, our results show that the adapted VRM through the cylinder volume formula is a valuable and reasonably reliable method for studying reduction intensity in early Upper

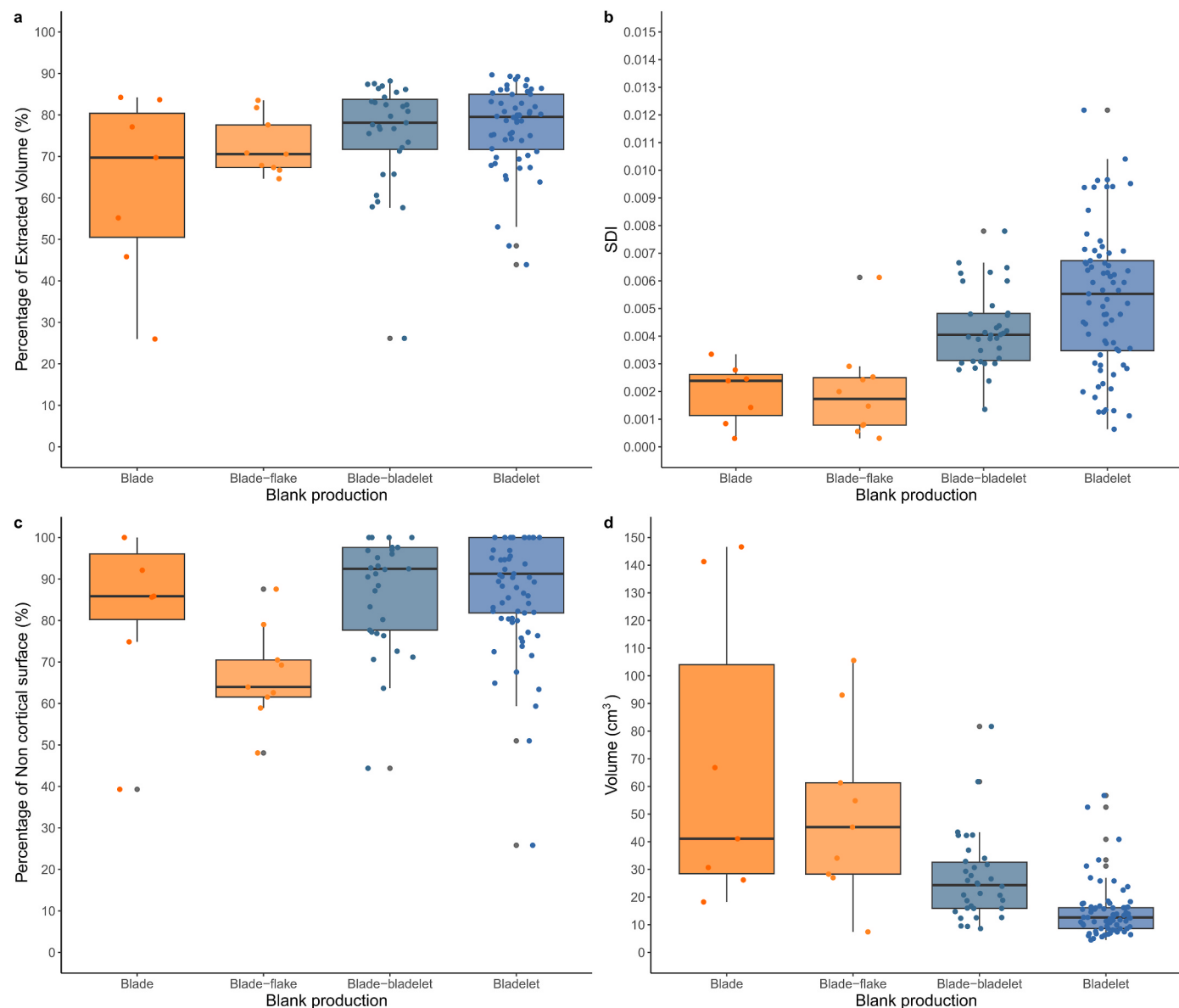


Fig. 9. Boxplots with jittered points showing the results for a) PEV obtained through VRM, b) SDI) c) Percentage of non-cortical surface, and d) volume of the cores according to blank production.

Paleolithic laminar assemblages. The different statistical tests performed (e.g., correlations, AE, MAE, and RMSE) show significant similarities between experimental data and the results of the reduction intensity quantifications obtained through the ellipsoid and cylinder geometric formulas. According to a Bland-Altman test, however, the cylinder formula is the one that most effectively reconstructs the original volume of these platform cores.

Interestingly, the results we obtained present a wider margin of error compared to the original version of the VRM (Lombao et al., 2020). This was expected and in our opinion, two main factors are responsible for that. First, the morphological and technological standardization of the reduction sequences in Protoaurignacian cores may require similar corrections units for the technical dimensions and thus limit original volume reconstructions (Lombao et al., 2020). Additionally, laminar technology is a recurrent reduction strategy in which multiple series of removals are detached either on a limited sector of the core or around its entire volume (Pigeot, 1987). This core volume management generates an overlapping effect that systematically eliminates information from previous phases; a characteristic that has been shown to negatively affect the performance of various reduction indexes (Lombao et al., 2019). On the other hand, the resolution of the volumetric reconstructions may have been affected by the high variability in the type and format of the starting raw materials. In this experiment, we used in fact a wide variety of core blanks (i.e., nodules and slabs) with very diverse starting morphologies and sizes. In some cases, we even used chunks resulting from the early phases of core decortication of a large-sized blank, with the aim of reproducing as closely as possible the archaeological evidence from Fumane.

Regarding the several variables tested in this experimental study, we observed a low effectiveness of multiple technological proxies to explore reduction intensity, such as the number of platforms, rotations, exploited surfaces, and convergences, as well as the resulting angle between flaking surfaces and striking platforms. This poor performance, which is well reflected in the low coefficients of determination, led us to exclude such variables in the following archaeological study. Instead, both the SDI and the non-cortical surface percentage showed higher coefficients of determination, as well as a high correlation with the VRM. However, some discrepancies were identified among these methods, particularly between the SDI and the VRM. Based on previous experimental works (Ditchfield, 2016; Lombao et al., 2019), it has been demonstrated that the SDI is significantly influenced by the size, specifically the volume, of the cores. Larger volumes tend to result in decreased SDI values, resulting in a lower perceived reduction intensity. Conversely, in the case of the VRM, the opposite trend may be observed: larger volumes lead to larger dimensions used in calculating the initial blank volume. This could potentially result in an overestimation of the reduction intensity, particularly for the initial cores.

Therefore, considering the discussed sources of error for the VRM and for the SDI, we highlight the importance of combining these three methods (VRM, SDI and non-cortical surface) for more effectively interpreting the archaeological data on reduction intensity, while evaluating and discussing potential discrepancies between them (Dibble, 1995b; Lombao et al., 2023b).

Table 7

Descriptive statistics for the percentage of extracted volume obtained through the VRM according to raw material. N = sample size. Min = minimum value, Max = maximum value, SD = Standard Deviation, CV = Coefficient of Variation, S-W = Shapiro-Wilk test. Shape (i.e., the degree of variability) and Scale (i.e., the rate of discard) values of the Weibull distribution for each Raw Material type, obtained with the data from the VRM analysis.

Raw material	N	Mean	Median	Min	Max	SD	CV	Shape	Scale
Maiolica	72	76.27	79.06	45.82	89.26	9.96	0.13	8.35	79.62
Other	2	88.02	88.02	86.38	89.67	2.32	0.03	16.53	94.85
Scaglia Rossa	6	77.56	74.86	68.27	89.32	8.33	0.11	7.88	85.56
Scaglia Variegata	8	67.40	71.47	25.99	87.03	19.67	0.29	3.83	75.44
Scaglia Variegata Type 3	15	71.45	77.12	26.14	88.57	16.32	0.23	5.79	78.67

4.2. Reduction intensity in the earliest protoaurignacian of Fumane Cave

After experimentally verifying the applicability of the reduction intensity methods to laminar cores, we proceeded to analyze core reduction intensity in the earliest Protoaurignacian assemblage from Fumane Cave to evaluate three key aspects of human technological behavior: 1) raw material management, 2) core technology strategies, and 3) the interrelationship between blade and bladelet productions along the reduction sequence. Results presented below are divided into these three themes.

4.2.1. Raw material

We found slight, but interesting variations in the management of raw materials. In particular, a few cores made from Maiolica show a lower volumetric depletion compared to the rest of the raw materials exploited at the site. We think that this is to be attributed to the greater abundance of the Maiolica in the area surrounding the site (Bertola, 2001). Previous studies have suggested that the Maiolica, together with the Scaglia Rossa and the Scaglia Variegata, were locally sourced, especially since most raw materials could be found within a few kilometers of the cave (Bertola, 2001; Delpiano et al., 2018). Such proximity and abundance are particularly marked for the Maiolica, thus resulting in a systematic transport of raw or tested cobbles and core blanks to the site for stone knapping, use, and discard. The preceding Mousterian and Uluzzian assemblages are comparable in this regard (Delpiano and Peresani, 2017; Peresani, 2012; Peresani et al., 2016). In the specific case of the A2–A1 assemblage, the presence of all phases of core reduction (e.g., fully cortical products, crested blades, and core tablets), as well as the high frequency of products with dorsal cortical surfaces, suggest that most of the decortication and initialization of cores was taking place in most cases at the site or close to the site. This is true for the Maiolica, Scaglia Rossa, and Scaglia Variegata, whereas the pattern is less clear for the more uncommon raw materials (Falcucci et al., 2017).

To this date, there is little information about the use of exogenous raw materials at Fumane, despite evidence of long-distance mobility and/or trade between geographically distant groups is attested by the abundance of marine shells recovered in the Protoaurignacian layers (Peresani et al., 2019). An exception to that is a handful of lithics made from a red radiolarite that is today found along the Lombardy Basin, at ca. 50 km west of the site (Bertola et al., 2013). This caption radius is nevertheless very limited if compared to the extensive raw material network reconstructed at the sites of Mochi and Bombrini in north-western Italy. Thanks to the varying frequencies of raw materials varieties from southeastern France and central Italy, both Grimaldi et al. (2014) and Riel-Salvatore and Negrino (2018) have been able to discuss the beginning of the Upper Paleolithic in the regions and explore the different mobility strategies undertaken by Protoaurignacian foragers throughout the development of the technocomplex. Applying the VRM to those case studies might prove to be ideal to further investigate mobility patterns in the region and correlate reduction intensity to distance of the different raw material sources.

The data available is still insufficient to quantitatively compare the economic management of lithic resources during the Mousterian with that of the Protoaurignacian at Fumane Cave through the reduction

intensity of cores or other lithic tools. However, despite the marked differences between the two technocomplexes, it is possible to point out a certain degree of similarity in techno-economic behaviors. First, there is a very similar pattern in terms of raw material transport strategies. For instance, in the A9 discoid Mousterian unit, dated to about 47.6–45.0 ky cal BP (Higham et al., 2009; Peresani et al., 2008), refits of specific sequences (Delpiano et al., 2017), as well as techno-economic studies carried out on the entire lithic assemblage (Delpiano et al., 2018), indicate a high degree of integrity of the reduction sequences in the case of local materials such as the Maiolica, suggesting a systematic production in the cave, or very close to it (Delpiano et al., 2018; Delpiano and Peresani, 2017). As we have seen, this element is present in the Protoaurignacian layers too, where we can also observe a less intense exploitation of this raw material type in some cores (Table 7).

Also, we can document in both archaeological units differential management of the raw materials according to their proximity, availability, and aptitude for knapping. In the A9 assemblage, it was suggested that a more planned behavior characterizes the use of semi-local materials, since those are introduced to perform specific tasks, and are reduced according to their different physical qualities (Delpiano et al., 2018). In this sense, this could be also deduced from the Protoaurignacian assemblage since we identified a greater degree of reduction in those semi-local raw materials of higher quality.

However, as noted by Peresani et al. (2016), considering the abundant use of fine-grained chert found in the vicinity of the cave, which is evident in the Protoaurignacian, Uluzzian, as well as across all the Mousterian sequence, the archaeological evidence from Fumane does not provide sufficient information to determine if there is a shift towards greater reliance on fine-grained, non-local raw materials as we move forward in time. It is important to note that the early Protoaurignacian assemblage at Fumane is a palimpsest due to complex site formation processes, making it challenging to distinguish individual occupation events. Different knapping strategies and the use of various raw material sources may have been influenced by diverse settlement dynamics during the formation of the stratigraphic unit. Achieving a more detailed resolution of this phase currently appears unlikely, a challenge frequently encountered in many Paleolithic cave contexts (Goldberg et al., 1993).

4.2.2. Core classification

Our sequential experiment exemplifies how cores undergo significant morphological variations throughout the core reduction sequence due to allometric modifications. This phenomenon has direct effects on the classification of cores into technological categories (see Falcucci and Peresani, 2018; Sánchez-Martínez et al., 2022), and the new reduction intensity data at Fumane reveals a clear pattern of transfer between core types.

Protoaurignacian foragers that visited the cave during the formation of unit A2–A1 exhibit a highly flexible operatory field (*sensu* Guilbaud, 1995), regarding the reduction sequence, with a predominance of a unidirectional concept of knapping along the longitudinal axes of the selected raw materials. Reduction sequences generally begin with a rough decortication of the core and the configuration of a flat and rather steep striking platform. In a few cases, crests could be prepared to allow the first laminar removal to be detached, but also to isolate the future flaking surface. Cores that display initialization procedures have generally few laminar removals visible and have been classified as initial cores in previous studies at the site. According to Falcucci and Peresani (2018), the knapping sequences were interrupted prior to the optimal production phase due to non-optimal flaking angles and distal convexities, as well as the concurrent formation of hinged removals on the flaking surface. Once the core was configured, two mutually exclusive options could occur, involving the exploitation of either a narrow or a wide surface.

There are some characteristic elements in the different core types identified that allow us to speak of distinct reduction procedures,

requiring specific morphological configurations. For instance, dorsal cresting is an operation carried out exclusively on narrow-sided cores to isolate the flaking surface and facilitate the removal of core tablets. Conversely, the core's inactive area lacks a specific configuration in the case of semicircumferential cores, characterized by the presence of removal scars located on at least two adjacent faces that progressively merge into a single convex surface (Falcucci and Peresani, 2018). However, our study indicates that the allometric changes, inherent to the reduction process, cause a transfer between core types. Depending on the perimetral development of the core's exploitation, both narrow- or wide-faced cores could evolve into semicircumferential cores. The latter would be thus the result of the extension of the knapping to the cores' flanks. This well-known semi-tournant pattern (Pigeot, 1987) allows for both maximized blank production and auto-maintainance of the convexities with a characteristic back and forth from the flanks to the center of the flaking surface.

Independently from the reduction taking place on a single or two adjacent surfaces (i.e., semicircumferential), the recurrent removal of products on narrow and semicircumferential cores will result in a morphological change into a typical wide-faced core. Interestingly, Falcucci and Peresani (2018) hypothesized that wide-faced cores are a direct result of a prolonged successful blank extraction from semicircumferential cores, which also complicates the determination of the blank selected as core (e.g., nodule, block, chunk), lacking cortical remains and other features useful to determine the blank type. This qualitative observation is now further supported by the quantitative data produced in this study, demonstrating how wide-faced cores have a higher percentage of extracted volume. Nevertheless, there are discrepancies among the reduction proxies. The SDI suggests that wide-faced cores exhibit lower reduction intensity compared to multiplatform and semicircumferential cores. However, this discrepancy may be attributed to the greater impact of negative overlap in wide-faced cores, as opposed to semicircumferential or multiplatform cores, or it could be due to the larger size of the core blanks, resulting in lower SDI values for wide-faced cores. A visual examination of the allometric changes of cores' platforms well exemplifies the shift from one type to another across one of our experimental reduction sequences (Fig. 10).

Despite the concept of equifinality being particularly important to better frame core reduction in the Protoaurignacian, the relationship between core types does not necessarily have to follow a linear transition from narrow-sided to semicircumferential cores or from semicircumferential to wide-faced types (Fig. 11). The exploitation strategy can be in fact constant throughout the reduction sequence without any significant volumetric change in the core, as attested by the estimated reduction intensity in some of the analyzed cores. Likewise, each knapping sequence has a distinct rhythm that does not always allow to distinguish the type of exploitation carried out by exclusively looking at the core at discard. A semicircumferential core could be for instance the result of two independent knapping series (e.g., one on a wide face and the other on a narrow face) that end up merging into one at an advanced stage of reduction. Only extensive refitting programs conducted on well-preserved sites would be able to notice such variations and more dynamically differentiate between different reduction procedures (see Romagnoli and Vaquero, 2019).

Overall, the unidirectional volumetric concept of knapping and the allometric changes across cores oriented according to their longitudinal axes (i.e., narrow-sided, semicircumferential, and wide-faced) indicate a certain technological fluidity that is a direct consequence of the reduction intensity. Having said that, allometric changes cannot explain all the technological variability described in the Protoaurignacian. Carinated cores, for instance, are characterized by a frontal flaking regression that penetrates orthogonally along the transversal axis of the blank (Falcucci and Peresani, 2018). From a theoretical point of view, it is possible that a morphological transfer occurs from semicircumferential to carinated cores. This is possible because, through reduction, several morphometric changes can occur. For instance, the volumetric features

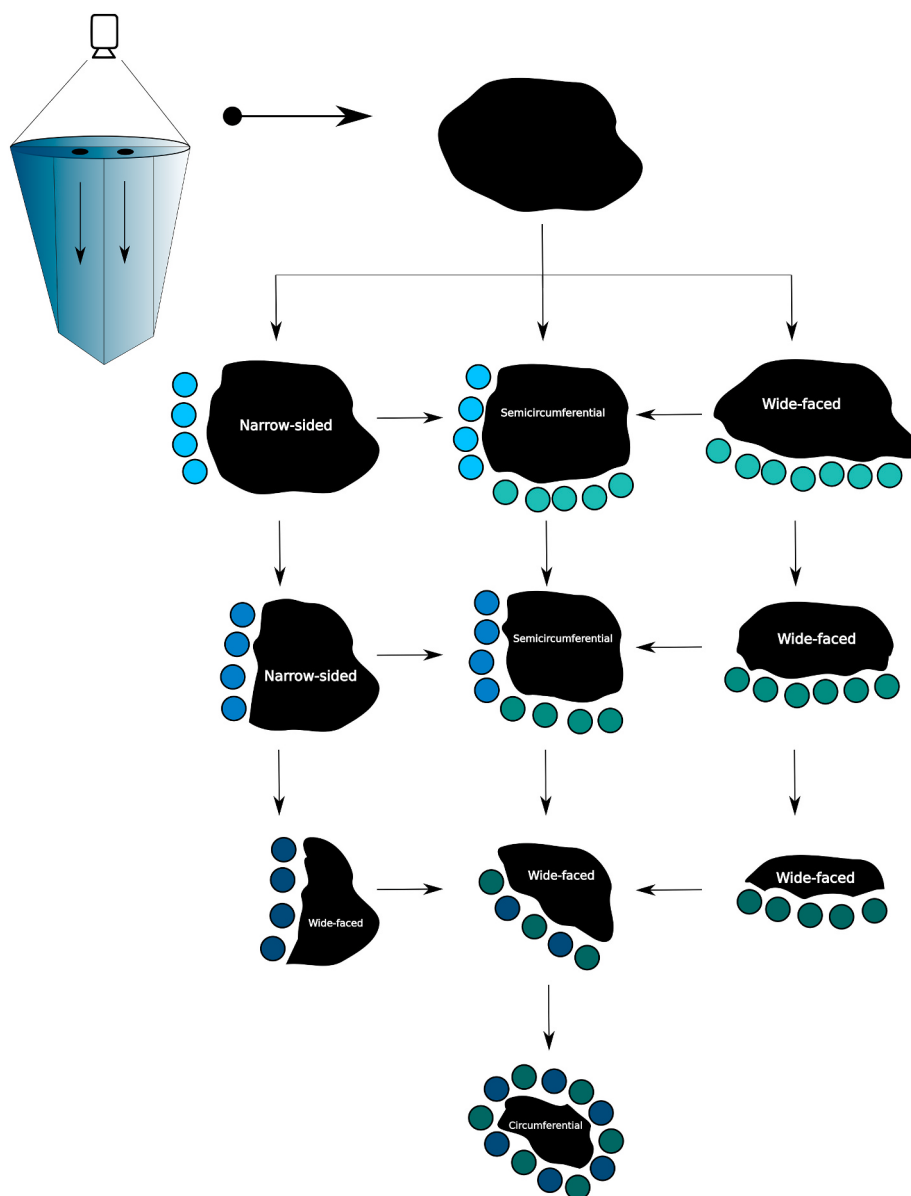


Fig. 10. Schematic drawings illustrating the interpretation of the operatory field inferred for the Protoaurignacian cores of Fumane Cave based on the findings of this study and the technological analysis of the assemblage. The blue dots display the progression of the knapping. (For interpretation of the references to color in this figure legend, the reader is referred to the Web version of this article).

of the core's flaking surface can be altered using flakes with plunging termination, whereas the longitudinal axis of the cores can drastically change when thick core tablets are removed.

However, several lines of evidence suggest that this occurrence is negligible. In the Aurignacian *sensu lato*, carinated cores are a well-defined technological category that is exclusively focused on obtaining rather short bladelets (Le Brun-Ricalens, 2005). At Fumane, the blanks selected for carinated technology are usually thick flakes, whose ventral sides are used as striking platforms and are almost never reshaped by total core tablets (Falcucci et al., 2017). These core types have been for a long time mistaken for thick endscrapers and the possibility that carinated pieces had a dual objective cannot be ruled out. This hypothesis has been for the time being dismissed at Fumane thanks to an extensive use-wear study of the endscrapers recovered across the Aurignacian sequence (Aleo et al., 2021).

Finally, multiplatform cores highlight the dynamic approach to core reduction of Protoaurignacian knappers aimed at maximizing raw material use. This technical solution allows knappers to overcome the loss

of ideal flaking convexities and striking angles by rotating the cores and opening new striking platforms. Volumetric re-organizations are usually not complex and can take advantage of the removals from the previous reduction phases to detach crest-like blanks, as well as using flat surfaces as striking platforms. At Fumane, these cores display in most cases two independent and consecutive unidirectional reduction sequences, although up to three successive platforms are attested (Falcucci and Peresani, 2018).

Our results suggest that most cores have been discarded at the site at an advanced stage of reduction, as indicated by both the percentages of extracted volume estimated from the VRM and the small size of the cores. Noteworthy is the fact that this high degree of reduction intensity also includes cores in the early stages of blank production. We can thus observe a rapid decrease in the volume of the cores already starting from the initial phases of the reduction sequence. All the steps related to the cores' volumetric configuration (e.g., decortication and opening of a striking platform) are very costly in terms of raw material, as suggested by Eren et al. (2008). Moreover, the previous studies at Fumane have

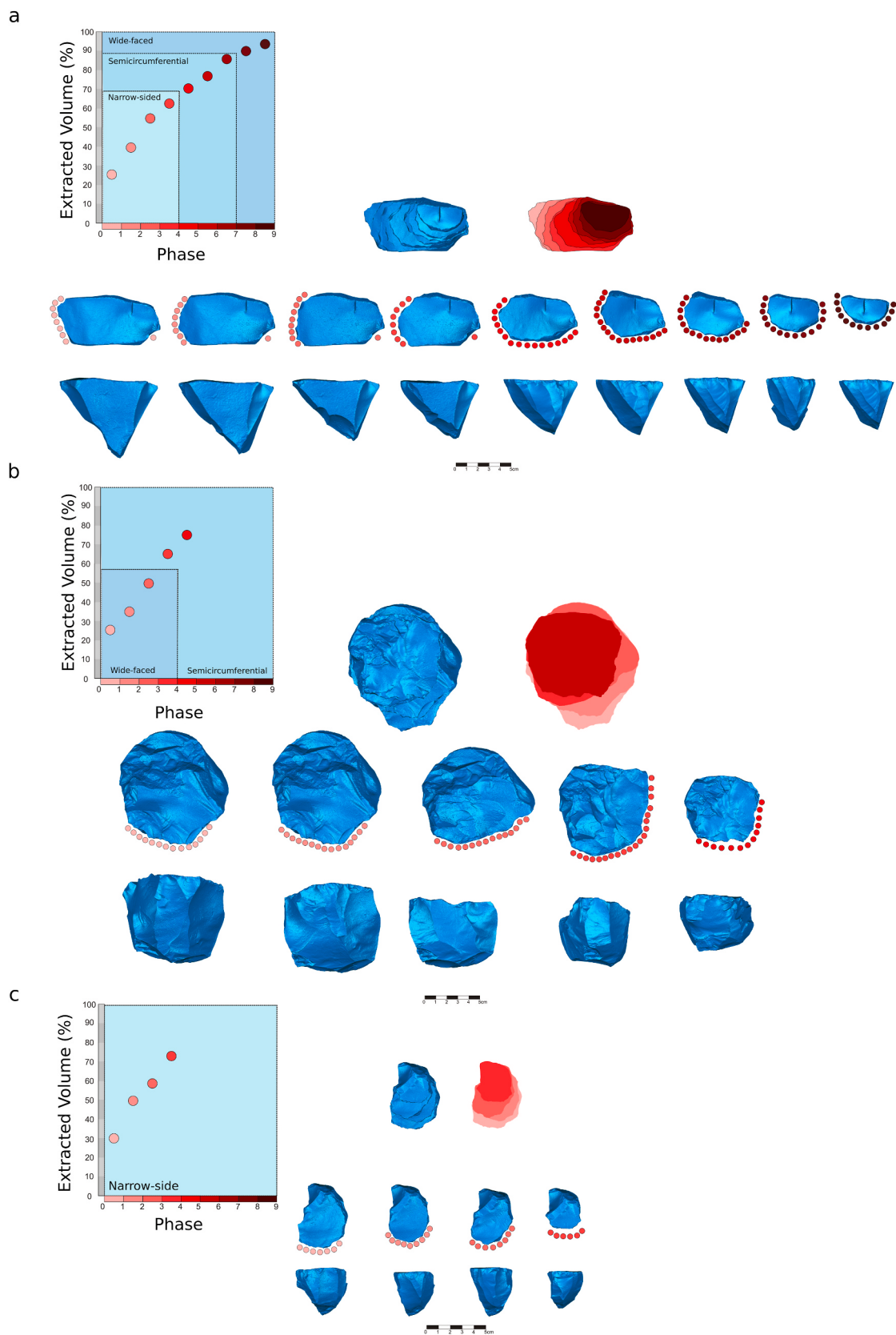


Fig. 11. Sequential phases of the core reduction sequences produced during the experiment with technological and morphological variations. The 3D models views are complemented by red dots around the striking platform marking blank removal areas. Left-side plots depict core type shifts relative to the percentage of extracted volume. A) Experimental core 1, B) Experimental core 4, C) Experimental core 99. (For interpretation of the references to color in this figure legend, the reader is referred to the Web version of this article).

underlined how core maintenance in the Protoaurignacian is very costly in terms of extracted volume (Falcucci et al., 2017; Falcucci and Peresani, 2018). While the VRM tends to overestimate the reduction intensity of cores in the early stages of reduction by approximately 10% of the percentage volume, the central values obtained for the initial cores remain close to 70%, with a range spanning from 25.9% to 86.2%. Accounting for this overestimation, the adjusted percentage falls to about 60% with a range of 15%–76%. Notably, this percentage aligns with the values obtained from the experimental cores used in this study. Specifically, the experimental cores reveal an actual reduction intensity in the first phase, recorded with a 3D scan after the first shaping-out removals, ranging from 21% to 48.8% of the extracted volume, with a median of 26%. This reduction intensity increases to a range of between 30% and 89.2% in the second phase, with a median of 43.9% (see Supplementary Table S6). These findings suggest a substantial loss of material in the initial phases of the reduction sequences, a quantitative observation that aligns with the available refits from Fumane.

4.2.3. Blank production

In this study, we have observed that, far from being watertight compartments, the core assemblage at Fumane Cave reflects a dynamic continuum either as a direct consequence of reduction or as a formal reorientation of the concept of knapping. These findings force us to rethink the benefits of classifying cores based on their shape at discard without taking into consideration their allometric relationships. In fact, a risky outcome of such a method would be to apply a typological approach to the results of dynamic knapping behaviors. In this framework, the discussion surrounding the production of blades and bladelets within a single core reduction sequence is also relevant. At Fumane, it can be safely stated that the main goal of blank production is to obtain bladelets, which is well evidenced by the greater quantity of bladelets, frequently modified by marginal retouch (Falcucci et al., 2018), and cores oriented toward their production. However, our results suggest a certain flexibility in production objectives, with a transition from blades to bladelets throughout the reduction sequence.

First, the reduction intensity data indicates a greater degree of reduction intensity in the cores oriented towards the production of bladelets, which is evidenced especially through the quantification of the SDI. It should be however mentioned that Lombao et al. (2019) have noticed how the SDI results may be influenced by differences in the size of the cores, which we can also notice in this study when looking at the inversely proportional relationship between volume and SDI values (see Fig. 9b,d). Nevertheless, the estimates obtained through the VRM support the evidence of a greater reduction intensity among bladelet cores, despite the results being less pronounced. A second element that allows us to infer a transition between production objectives is the differential presence of cortex on the dorsal face of blades and bladelets. More specifically, blades with cortical surfaces represent around 28% of the total blade category, while the frequency drastically decreases to 6% in the case of bladelets. This suggests that many of the blades discarded at the site were produced in the early phases of the reduction sequences when a complete decortication of the core had not yet been achieved.

The presence of both blade and bladelet scars in some cores points to a certain degree of flexibility in exploitation objectives. The removal of blades can also occur among bladelet-oriented cores to maintain both the distal and lateral cores' convexities (Falcucci et al., 2017). These actions result in a certain subordination of blades to the production of bladelets, without a proper linear shift of production objectives throughout the reduction sequence. Simultaneous production is thus a well-described behavior that is also reflected in the use of maintenance blades to manufacture common tools such as endscrapers and burins. In the same way as with core types, the allometric changes produced by the volumetric depletion of the cores through the reconfiguration of striking platforms and distal convexities can be responsible for the modification of the production objectives. This flexibility in production objectives is thus consistent with the flexibility recorded in the type of exploitation.

Other elements point to a certain degree of independence between the two objectives of exploitation. Among them, the high degree of reduction of all cores, regardless of the scars visible at discard, should be highlighted, indicating that the exploitation of blades remains constant throughout the sequence. The refit of the blade core presented by Falcucci et al. (2017) is a fitting example of this observation. Secondly, the existence of types of exploitation oriented exclusively towards the exploitation of bladelets, such as in the case of carinated cores, indicates that bladelets are the sole objective of this reduction strategy from the initial moments of the sequence (Falcucci and Peresani, 2018). Moreover, narrow-sided cores are exclusively oriented towards the production of bladelets and present a lower degree of general reduction intensity compared to other core types, thus indicating the production of bladelets from the early stages of the reduction sequence. This observation is however not straightforward, as our results underline how the production of blades based on narrow-sided cores might have occurred in earlier stages of reduction; or in other words before the core went through a morphological reorganization, thus changing the type of exploitation (i.e., semicircumferential) or the goals.

The combination of reduction intensity methods and the previous technological observations at Fumane (e.g., Bertola et al., 2013; Falcucci et al., 2017) permit us to observe at a general level that two different patterns in the production of blades and bladelets exist. On one hand, there is a production aimed at obtaining exclusively bladelets, while on the other hand, a more flexible production that sees either a linear change in knapping objectives as reduction increases or an alternation in the production of blanks of different sizes that are commonly lumped into the categories of blades and bladelets. In the latter case, bladelets would be the main objective of the exploitation, while blades would correspond to secondary productions resulting from the cores' reconditioning operations. From a morphological standpoint, bladelets appear to be more standardized than blades, as demonstrated thanks to three-dimensional geometric morphometric approaches (Falcucci et al., 2022; Falcucci and Peresani, 2022). This increased standardization in bladelet production is expected since functional studies indicate that these products were mounted in series along the shafts of composite tools (Broglio et al., 2005; Porraz et al., 2010; Rios-Garaizar, 2012) whereas knappers selected blades to manufacture tools for which characteristics such as the robustness were more important than shape (Aleo et al., 2021). In this framework, the Protoaurignacian appears to be a highly effective adaptive system that could well cope with different environmental settings and climatic shifts, as suggested by Riel-Salvatore and Negrino (2018). Future discussions concerning this cultural variant should prioritize the dynamic evidence presented by core reduction intensity assessments, rather than exclusively concentrating on the classification of blank and core types based on their size and shape. This approach will allow for a more comprehensive exploration of Aurignacian economic behavior over time and across regions. The growing body of evidence suggests that throughout the Upper Paleolithic, there was an increase in lithic miniaturization. This phenomenon is closely related to human strategies for adapting to changing environments, as well as the mobility and settlement dynamics of highly mobile foraging groups (Kuhn, 2020; Kuhn and Shimelmitz, 2023; Pargeter and Shea, 2019).

Likewise, reduction intensity studies should be extended to pivotal Early Aurignacian sites to assess whether behind the high prevalence of carinated cores there exists a specific technological behavior finalized at maximizing blank production within an increasingly mobile human settlement strategy, which has also been associated with an expansion of the ecological niche in response to environmental deterioration (Banks et al., 2013).

5. Conclusions

This study has provided a platform to explore reduction intensity within the earliest Protoaurignacian lithic assemblage at Fumane Cave.

Despite its significant relevance to discussions on technological variability and human behavior, reduction intensity is often overlooked in Upper Paleolithic studies. In this paper, we present archaeological findings supported by a sequential knapping experiment built upon 3D scanning technology. This experiment enabled us to evaluate the performance of the VRM (Lombao et al., 2020) on blade and bladelet cores, while also incorporating other measures of reduction intensity, such as the SDI by Clarkson (2013). Analyzing laminar cores presents particular challenges due to their high standardization and the systematic removal of products along a relatively stable morphological axis. Nevertheless, the results of our experimental study are highly promising, and this adapted VRM method holds great potential for further investigations into reduction intensity within Upper Paleolithic assemblages. To facilitate future research, we have compiled a step-by-step R Markdown file and shared all experimental and archaeological data underlying our findings (Falcucci and Peresani, 2023; Lombao et al., 2023a), streamlining the application of this method with minimal data preparation efforts.

At Fumane Cave, we have addressed three research questions related to reduction intensity, examining variations in raw material exploitation within the Protoaurignacian, the technological classification of cores, and the interrelationships between blade and bladelet productions. Regarding raw material management, we have identified subtle differences in reduction intensity based on the abundance and proximity of available raw materials. The Maiolica emerges as the most abundant variety and exhibits the largest number of less reduced cores. The identified variability within the operatory field and the production of blades and bladelets exemplifies the complex and adaptable nature of human behavior. In this context, a clear separation between the operatory fields of blade and bladelet productions cannot be established due to the scarcity of cores dedicated exclusively to blade production, the simultaneous production of blades and bladelets from the same cores, and the shift from blade to bladelet production after the initial phases of reduction. In conclusion, this paper underscores the critical role of incorporating the temporal dimension, particularly through the assessment of reduction intensity, in the study of stone tool production. This approach will allow archaeologists to unravel subtle variations across both space and time, thereby facilitating the testing of more compelling hypotheses regarding the development of the Upper Paleolithic and the adaptive behaviors of *Homo sapiens* in the diverse ecological settings of Europe.

CRediT authorship contribution statement

Diego Lombao: Conceptualization, Methodology, Software, Validation, Formal analysis, Investigation, Resources, Data curation, Writing – original draft, Writing – review & editing, Visualization, Funding acquisition. **Armando Falcucci:** Conceptualization, Methodology, Validation, Formal analysis, Investigation, Resources, Data curation, Visualization, Supervision, Funding acquisition, Writing – original draft, Writing - review & editing. **Elena Moos:** Investigation. **Marco Peresani:** Resources, Writing – review & editing, Funding acquisition.

Declaration of competing interest

The authors declare that they have no known competing financial interests or personal relationships that could have appeared to influence the work reported in this paper

Acknowledgments

This study was supported by the German Research Foundation (DFG) under grant agreement no. 431809858 (project title: “Investigating Early Upper Paleolithic Technological Variability and Cultural Dynamics South of the Alps”; recipient: A.F.). Fieldwork and research at

Fumane Cave are coordinated by the Ferrara University (M.P.), with the collaboration of Italian and European research centers and with the support of the Ministry of Cultural Heritage, Archaeological Superintendence SAPAB, public institutions (Lessinia Regional Natural Park, B. I.M. Adige, Municipality of Fumane), private associations, and companies. D.L. was supported by a postdoctoral Xunta de Galicia grant (ED481B-2022-048). The Institut Català de Paleoecologia Humana i Evolució Social (IPHES-CERCA) received financial support from the Spanish Ministry of Science and Innovation through the “María de Maeztu” program for Units of Excellence (CEX-2019-000945-M). We would like to acknowledge all the researchers and students who have been actively engaged in the recovery, preparation, and study of the archaeological record from Fumane Cave throughout the years of research at this site. Finally, we thank D. Delpiano for providing us with some of the nodules used in the knapping experiment.

Appendix A. Supplementary data

Supplementary data to this article can be found online at <https://doi.org/10.1016/j.jas.2023.105889>.

References

- Abulafia, T., Goder-Goldberger, M., Berna, F., Barzilai, O., Marder, O., 2021. A technotypological analysis of the Ahmarian and Levantine Aurignacian assemblages from Manot Cave (area C) and the interrelation with site formation processes. *J. Hum. Evol.* 160, 102707 <https://doi.org/10.1016/j.jhevol.2019.102707>.
- Aleo, A., Duches, R., Falcucci, A., Rots, V., Peresani, M., 2021. Scraping hide in the early upper paleolithic: insights into the life and function of the protoaurignacian endscrapers at Fumane cave. *Archaeol. Anthropol. Sci.* 13, 137. <https://doi.org/10.1007/s12520-021-01367-4>.
- Andrefsky, W.J., 1994. Raw-material availability and the organization of technology. *Am. Antiq.* 59, 21–34.
- Arrizabalaga, A., Altuna, J., 2000. *Labeko Koba (País Vasco). Hienas y humanos en los albores del Paleolítico superior*. Munibe 52.
- Bailey, S.E., Weaver, T.D., Hublin, J.-J., 2009. Who made the Aurignacian and other early Upper Paleolithic industries? *J. Hum. Evol.* 57, 11–26. <https://doi.org/10.1016/j.jhevol.2009.02.003>.
- Banks, W.E., D'Errico, F., Zilhão, J., 2013. Human–climate interaction during the early upper paleolithic: testing the hypothesis of an adaptive shift between the proto-aurignacian and the early aurignacian. *J. Hum. Evol.* 64, 39–55. <https://doi.org/10.1016/j.jhevol.2012.10.001>.
- Barshay-Szmidt, C., Eisenberg, L., Deschamps, M., 2013. Radiocarbon (AMS) dating the classic aurignacian, proto-aurignacian and vasconian moustierian at gatzarría cave (Pyrénées-Atlantiques, France). *Paléo* 23, 11–38.
- Barshay-Szmidt, C., Normand, C., Flas, D., Soulier, M.-C., 2018. Radiocarbon dating the aurignacian sequence at Isturitz (France): implications for the timing and development of the protoaurignacian and early aurignacian in western Europe. *J. Archaeol. Sci. Reports* 17, 809–838. <https://doi.org/10.1016/j.jasrep.2017.09.003>.
- Bartolomei, G., Broglia, A., Cassoli, P.F., Castelletti, L., Cattani, L., Cremaschi, M., Giacobini, G., Malerba, G., Maspero, A., Peresani, M., Sartorelli, A., Tagliacozzo, A., 1992. La Grotte de Fumane. Un site aurignacien au pied des Alpes. *Preistoria Alp.* 28, 131–179.
- Barton, C.M., Riel-Salvatore, J., 2014. The formation of lithic assemblages. *J. Archaeol. Sci.* 46, 334–352. <https://doi.org/10.1016/j.jas.2014.03.031>.
- Bataille, G., 2017. Extracting the “Proto” from the Aurignacian. Distinct production sequences of blades and bladelets in the lower Aurignacian phase of Siuren I, units H and G (Crimea). *Mitteilungen der Gesellschaft für Urgeschichte* 25, 49–85.
- Bataille, G., Conard, N.J., 2018. Blade and bladelet production at holle fels cave, AH IV in the swabian Jura and its importance for characterizing the technological variability of the aurignacian in central Europe. *PLoS One* 13, e0194097. <https://doi.org/10.1371/journal.pone.0194097>.
- Bataille, G., Falcucci, A., Tafelmaier, Y., Conard, N.J., 2020. Technological differences between Kostenki 17/II (Spitsynskaya industry, Central Russia) and the Protoaurignacian: reply to Dinnis et al. *J. Hum. Evol.* 146, 102685 <https://doi.org/10.1016/j.jhevol.2019.102685>, 2019.
- Benazzi, S., Douka, K., Fornai, C., Bauer, C.C., Kullmer, O., Svoboda, J., Pap, I., Mallegni, F., Bayle, P., Coquerelle, M., Condemi, S., Ronchitelli, A., Harvati, K., Weber, G.W., 2011. Early dispersal of modern humans in Europe and implications for Neanderthal behaviour. *Nature* 479, 525–528. <https://doi.org/10.1038/nature10617>.
- Benazzi, S., Slon, V., Talamo, S., Negrino, F., Peresani, M., Bailey, S.E., Sawyer, S., Panetta, D., Vicino, G., Starnini, E., Mannino, M.A., Salvadori, P.A., Meyer, M., Paabo, S., Hublin, J.-J., 2015. The makers of the Protoaurignacian and implications for Neanderthal extinction. *Science* 348, 793–796. <https://doi.org/10.1126/science.aaa2773>.

- Bertola, S., 2001. Contributo allo studio del comportamento dei primi gruppi di *Homo sapiens sapiens* diffusi in Europa (PhD Thesis). In: Sfruttamento della selce, produzione dei supporti lamellari, confezione delle armature litiche nel sito aurignaziano della Grotta di Fumane nei Monti Less. University of Bologna.
- Bertola, S., Broglio, A., Cristiani, E., De Stefani, M., Gurioli, F., Negrino, F., Romandini, M., Vanhaeren, M., 2013. La diffusione del primo Aurignaziano a sud dell'arco alpino. *Preistoria Alp.* 47, 123–152.
- Blades, B.S., 2003. End scraper reduction and hunter-gatherer mobility. *Am. Antiqu.* 68, 141–156.
- Bland, J.M., Altman, D.G., 1995. Comparing methods of measurement: why plotting difference against standard method is misleading. *Lancet* 346, 1085–1087. [https://doi.org/10.1016/S0140-6736\(95\)91748-9](https://doi.org/10.1016/S0140-6736(95)91748-9).
- Bon, F., 2006. A brief overview of Aurignacian cultures in the context of the industries of the transition from the Middle to the Upper Paleolithic. In: Bar-Yosef, O., Zilhão, J. (Eds.), Proceedings of the Symposium "Towards a Definition of the Aurignacian, vol. 45. Trabalhos de Arqueologia, Lisbon, pp. 133–144.
- Bon, F., 2005. Little big tool. Enquête autour du succès de la lame. In: Le Brun-Ricalens, F. (Ed.), Productions Lamellaires Attribuées à l'Aurignacien. MNHA, Luxembourg, pp. 479–484.
- Bon, F., 2002a. Les termes de l'Aurignacien. In: Bon, F., Maillot-Fernández, J.M., Cobos i Ortega, D. (Eds.), Autour Des Concepts de Protoaurignacien, d'Aurignacien Archaique, Initial et Ancien. Unité et Variabilité Des Comportements Techniques Des Premiers Groupes d'hommes Modernes Dans Le Sud de La France et Le Nord de l'Espagne. Espacio, Tiempo y Forma, Serie I - Prehistoria y Arqueología 15. Universidad Nacional de Educación a Distancia, Madrid, pp. 39–64.
- Bon, F., 2002b. L'Aurignacien entre mer et océan: réflexion sur l'unité des phases anciennes de l'Aurignacien dans le Sud de la France. Société préhistorique française, Paris.
- Bon, F., Bodu, P., 2002. Analyse technologique du débitage aurignacien. In: Schmider, B. (Ed.), L'Aurignacien de La Grotte Du Renne Les Fouilles d'André Leroi-Gourhan à Arcy-Sur-Cure (Yonne). CNRS, Paris, pp. 115–133.
- Bon, F., Teysandier, N., Bordes, J.-G., 2010. La signification culturelle des équipements lithiques. In: Otte, M. (Ed.), Les Aurignaciens. éditions errance, Paris, pp. 45–65.
- Bordes, J.-G., 2005. La séquence aurignacienne du Nord de l'Aquitaine: variabilité des productions lamellaires à Caminade-Est, roc-de- Combe, Le Piage et Corbiac-Vignoble II. In: Le Brun-Ricalens, F. (Ed.), Productions Lamellaires Attribuées à l'Aurignacien: Chaînes Opératoires et Perspectives Technoculturelles. MNHA, Luxembourg, pp. 123–154.
- Broglio, A., Bertola, S., de Stefani, M., Marini, D., Lemorini, C., Rossetti, P., 2005. La production lamellaire et les armatures lamellaires de l'Aurignacien ancien de la grotte de Fumane (Monte Lessini, Vénétie). In: Brun-Ricalens, L.F. (Ed.), Productions Lamellaires Attribuées à l'Aurignacien. MNHA, Luxembourg, pp. 415–436.
- Bustos-Pérez, G., Baena, J., 2019. Exploring volume lost in retouched artifacts using height of retouch and length of retouched edge. *J. Archaeol. Sci. Reports* 27, 101922. <https://doi.org/10.1016/j.jasrep.2019.101922>.
- Carr, P.J., Bradbury, A.P., 2011. Learning from lithics: a perspective on the foundation and future of the organisation of technology. *PaleoAnthropology* 305–319. <https://doi.org/10.4207/PA.2011.ART61>.
- Chu, W., 2018. The Danube corridor hypothesis and the carpathian basin: geological, environmental and archaeological approaches to characterizing aurignacian dynamics. *J. World PreHistory* 31, 117–178. <https://doi.org/10.1007/s10963-018-9115-1>.
- Cignoni, P., Callieri, M., Corsini, M., Dellepiane, M., Ganovelli, F., Ranzuglia, G., 2008. MeshLab: an open-source mesh processing tool. In: Scaramo, V., Chiara, R. De, Erra, U. (Eds.), Eurographics Italian Chapter Conference. The Eurographics Association, pp. 129–136. <https://doi.org/10.2312/LocalChapterEvents/ItalChap/ItalianChapConf2008/129-136>.
- Clarkson, C., 2013. Measuring core reduction using 3D flake scar density : a test case of changing core reduction at Klasies River Mouth , South Africa. *J. Archaeol. Sci.* 40, 4348–4357. <https://doi.org/10.1016/j.jas.2013.06.007>.
- Conard, N.J., Bolus, M., 2008. Radiocarbon dating the late middle paleolithic and the aurignacian of the swabian Jura. *J. Hum. Evol.* 55, 886–897. <https://doi.org/10.1016/j.jhevol.2008.08.006>.
- Conard, N.J., Bolus, M., 2006. The swabian aurignacian and its place in European prehistory. In: Bar-Josef, O., Zilhão, J. (Eds.), Towards a Definition of the Aurignacian. IPA, Lisbon, pp. 219–239.
- Conard, N.J., Bolus, M., 2003. Radiocarbon dating the appearance of modern humans and timing of cultural innovations in Europe: new results and new challenges. *J. Hum. Evol.* 44, 331–371. [https://doi.org/10.1016/S0047-2484\(02\)00202-6](https://doi.org/10.1016/S0047-2484(02)00202-6).
- Cueva-Temprana, A., Lombao, D., Soto, M., Itambu, M., Bushozi, P., Boivin, N., Petraglia, M., Mercader, J., 2022. Oldowan technology amid shifting environments ~2.03–1.83 million years ago. *Front. Ecol. Evol.* 10 <https://doi.org/10.3389/fevo.2022.78810>.
- d'Errico, F., Borgia, V., Ronchitelli, A., 2012. Uluzzian bone technology and its implications for the origin of behavioural modernity. *Quat. Int.* 259, 59–71. <https://doi.org/10.1016/j.quaint.2011.03.039>.
- Davies, W., 2007. Re-evaluating the Aurignacian as an expression of modern human mobility and dispersal. In: Mellars, P., Boyle, K., Bar-Yosef, O., Stringer, C. (Eds.), Rethinking the Human Revolution: New Behavioural and Biological Perspectives on the Origin and Dispersal of Modern Humans. McDonald Institute for Archaeological Research, Cambridge, pp. 263–274.
- Davis, W., Hedges, R., 2008. Dating a type site: fitting Szeleta Cave into its regional chronometric context. *Præhistoria* 9 (10), 35–45.
- de Sonneville-Bordes, D., 1983. L'évolution des industries aurignaciennes. In: Aurignacien et Gravettien en Europe. ERAUL, Liège.
- de Sonneville-Bordes, D., 1960. Le Paléolithique supérieur en Périgord. Delmas, Bordeaux.
- Delignette-Muller, M.L., Dutang, C., 2015. Fitdistrplus: an R package for fitting distributions. *J. Stat. Software* 64, 1–34.
- Delpiano, D., Heasley, K., Peresani, M., 2018. Assessing Neanderthal land use and lithic raw material management in Discoid technology. *J. Anthropol. Sci.* 31, 89–110. <https://doi.org/10.4436/JASS.96006>.
- Delpiano, D., Peresani, M., 2017. Exploring Neanderthal skills and lithic economy. The implication of a refitted Discoid reduction sequence reconstructed using 3D virtual analysis. *Comptes Rendus Palevol* 16, 865–877. <https://doi.org/10.1016/j.crpv.2017.06.008>.
- Delpiano, D., Peresani, M., Pastoors, A., 2017. The contribution of 3D visual technology to the study of Palaeolithic knapped stones based on refitting. *Digit. Appl. Archaeol. Cult. Herit.* 4, 28–38. <https://doi.org/10.1016/j.daach.2017.02.002>.
- Delporte, H., 1991. La séquence aurignacienne et périgordienne sur la base des travaux récents réalisés en Périgord. *Bull. la Société Préhistorique Française* 88, 243–256.
- Demars, P.Y., 1992. L'Aurignacien ancien en Périgord: le problème du Protoaurignacien. *Paléo* 4, 101–122.
- Dibble, H.L., 1995a. Biache saint-vaast, level iiia: a comparison of analytical approaches. In: Dibble, H.L., Bar-Yosef, O. (Eds.), The Definition and Interpretation of Levallois Technology. Monographs in World Archaeology, vol. 23. Prehistory Press, Madison, pp. 93–116.
- Dibble, H.L., 1995b. Raw material availability, intensity of utilization and middle paleolithic assemblage variability. In: Dibble, H.L., Lenoir, M. (Eds.), The Middle Paleolithic Site of Combe-Capelle Bas (France). University Museum Press, Philadelphia, pp. 289–315.
- Dinnis, R., Bessudnov, A., Chiotti, L., Flas, D., Michel, A., 2019. Thoughts on the structure of the European aurignacian, with particular focus on hohle fels IV. *Proc. Prehist. Soc.* 85, 29–60. <https://doi.org/10.1017/ppr.2019.11>.
- Ditchfield, K., 2016. The influence of raw material size on stone artefact assemblage formation: an example from Bone Cave, south-western Tasmania. *Quat. Int.* 422, 29–43. <https://doi.org/10.1016/j.quaint.2016.03.013>.
- Dorner, W.W., 1999. Using microsoft excel for Weibull analysis. *Quality Digest* 19. Qual. Dig. 19, 33–41.
- Douglass, M.J., Lin, S.C., Braun, D.R., Plummer, T.W., 2018. Core use-life distributions in lithic assemblages as a means for reconstructing behavioral patterns. *J. Archaeol. Method Theory* 25, 254–288. <https://doi.org/10.1007/s10816-017-9334-22>.
- Douka, K., Grimaldi, S., Boschin, G., del Lucchese, A., Higham, T.F.G., 2012. A new chronostratigraphic framework for the upper palaeolithic of riparo Mochi (Italy). *J. Hum. Evol.* 62, 286–299. <https://doi.org/10.1016/j.jhevol.2011.11.009>.
- Dujardin, V., 2001. Sondages à La Quina aval (Gardes-le-Pontaroux, Charente, France). *Antiq. Ant.* 33, 21–26.
- Eren, M.I., Domínguez-Rodrigo, M., Kuhn, S.L., Adler, D.S., Le, I., Bar-Yosef, O., 2005. Defining and measuring reduction in unifacial stone tools. *J. Archaeol. Sci.* 32, 1190–1201. <https://doi.org/10.1016/j.jas.2005.03.003>.
- Eren, M.I., Greenspan, A., Sampson, C.G., 2008. Are Upper Paleolithic blade cores more productive than Middle Paleolithic discoidal cores? A replication experiment. *J. Hum. Evol.* 55, 952–961. <https://doi.org/10.1016/j.jhevol.2008.07.009>.
- Eren, M.I., Sampson, C.G., 2009. Kuhn's geometric Index of unifacial stone tool reduction (GIUR): does it measure missing flake mass? *J. Archaeol. Sci.* 36, 1243–1247. <https://doi.org/10.1016/j.jas.2009.01.011>.
- Falcucci, A., Conard, N.J., Peresani, M., 2020. Breaking through the Aquitaine frame: a re-evaluation on the significance of regional variants during the Aurignacian as seen from a key record in southern Europe. *J. Anthropol. Sci.* 98, 99–140. <https://doi.org/10.4436/JASS.98021>.
- Falcucci, A., Conard, N.J., Peresani, M., 2017. A critical assessment of the Protoaurignacian lithic technology at Fumane Cave and its implications for the definition of the earliest Aurignacian. *PLoS One* 12, e0189241. <https://doi.org/10.1371/journal.pone.0189241>.
- Falcucci, A., Karakostis, F.A., Göldner, D., Peresani, M., 2022. Bringing shape into focus: assessing differences between blades and bladelets and their technological significance in 3D form. *J. Archaeol. Sci. Reports* 43, 103490. <https://doi.org/10.1016/j.jasrep.2022.103490>.
- Falcucci, A., Peresani, M., 2023. The Open Aurignacian Project, vol. 1. <https://doi.org/10.5281/zenodo.6362149>. Fumane Cave in northeastern Italy (v.2.1.1). Zenodo.
- Falcucci, A., Peresani, M., 2022. The contribution of integrated 3D model analysis to Protoaurignacian stone tool design. *PLoS One* 17, e0268539. <https://doi.org/10.1371/journal.pone.0268539>.
- Falcucci, A., Peresani, M., 2018. Protoaurignacian core reduction procedures: blade and bladelet technologies at Fumane cave. *Lithic Technol.* 43, 125–140. <https://doi.org/10.1080/01977261.2018.1439681>.
- Falcucci, A., Peresani, M., Roussel, M., Normand, C., Soressi, M., 2018. What's the point? Retouched bladelet variability in the protoaurignacian. Results from Fumane, Isturitz, and les cottés. *Archaeol. Anthropol. Sci.* 10, 539–554. <https://doi.org/10.1007/s12520-016-0365-5>.
- Frouin, M., Douka, K., Dave, A.K., Schwenninger, J.-L., Mercier, N., Murray, A.S., Santaniello, F., Boschin, G., Grimaldi, S., Higham, T., 2022. A refined chronology for the middle and early upper paleolithic sequence of riparo Mochi (liguria, Italy). *J. Hum. Evol.* 69, 103211. <https://doi.org/10.1016/j.jhevol.2022.103211>.
- Goldberg, P., Nash, D.T., Petraglia, M., 1993. Formation Processes in Archaeological Context. Prehistory Press, Madison.
- Göldner, D., Karakostis, F.A., Falcucci, A., 2022. Practical and technical aspects for the 3D scanning of lithic artefacts using micro-computed tomography techniques and laser light scanners for subsequent geometric morphometric analysis. Introducing the StyroStone protocol. *PLoS One* 17, e0267163. <https://doi.org/10.1371/journal.pone.0267163>.

- Grimaldi, S., Porraz, G., Santaniello, F., 2014. Raw material procurement and land use in the northern mediterranean arc: insight from the first proto-aurignacian of riparo Mochi (balzi rossi, Italy). *Quartar* 61, 113–127. https://doi.org/10.7485/QU61_06.
- Guilbaud, M., 1995. *Introduction sommaire au concept de champ opératoire*. Cah. Noir 7, 121–133.
- Guilbaud, M., 1993. Debitage from the upper castelperronian level at saint-césaire. In: Lévéque, F., Backer, A.M., Guilbaud, M. (Eds.), *Context of a Late Neandertal: Implications of Multidisciplinary Research for the Transition to Upper Paleolithic Adaptations at Saint Césaire, Charente-Maritime, France*. Prehistory Press, Madison, pp. 37–58.
- Harvati, K., Röding, C., Bosman, A.M., Karakostis, F.A., Grün, R., Stringer, C., Karkanas, P., Thompson, N.C., Koutoulidis, V., Moulopoulos, L.A., Gorgoulis, V.G., Koulikoussa, M., 2019. Apidima Cave fossils provide earliest evidence of Homo sapiens in Eurasia. *Nature* 571, 500–504. <https://doi.org/10.1038/s41586-019-1376-z>.
- Haws, J.A., Benedetti, M.M., Talamo, S., Bicho, N., Cascalheira, J., Ellis, M.G., Carvalho, M.M., Friedl, L., Pereira, T., Zinsius, B.K., 2020. The early Aurignacian dispersal of modern humans into westernmost Eurasia. *Proc. Natl. Acad. Sci. USA* 117, 25414–25422. <https://doi.org/10.1073/pnas.2016062117>.
- Higham, T., Basell, L., Jacobi, R., Wood, R., Ramsey, C.B., Conard, N.J., 2012. Testing models for the beginnings of the Aurignacian and the advent of figurative art and music: the radiocarbon chronology of Geißenklösterle. *J. Hum. Evol.* 62, 664–676. <https://doi.org/10.1016/j.jhevol.2012.03.003>.
- Higham, T., Brock, F., Peresani, M., Brogiolo, A., Wood, R., Douka, K., 2009. Problems with radiocarbon dating the middle to upper palaeolithic transition in Italy. *Quat. Sci. Rev.* 28, 1257–1267. <https://doi.org/10.1016/j.quascirev.2008.12.018>.
- Higham, T., Douka, K., Wood, R., Ramsey, C.B., Brock, F., Basell, L., Camps, M., Arrizabalaga, A., Baena, J., Barroso-Ruiz, C., Bergman, C., Boitard, C., Boscato, P., Caparrós, M., Conard, N.J., Draily, C., Froment, A., Galván, B., Gambassini, P., García-Moreno, A., Grimaldi, S., Haesaerts, P., Holt, B., Iriarte-Chiapuso, M.-J., Jelinek, A., Jordá Pardo, J.F., Maillo-Fernández, J.-M., Marom, A., Maroto, J., Menéndez, M., Metz, L., Morin, E., Moroni, A., Negrino, F., Panagopoulou, E., Peresani, M., Pirson, S., de la Rasilla, M., Riel-Salvatore, J., Ronchitelli, A., Santamaría, D., Semal, P., Slimak, L., Soler, N., Villaluenga, A., Pinhasi, R., Jacobi, R., 2014. The timing and spatiotemporal patterning of Neanderthal disappearance. *Nature* 512, 306–309. <https://doi.org/10.1038/nature13621>.
- Hofecker, J.F., 2009. The spread of modern humans in Europe. *Proc. Natl. Acad. Sci. USA* 106, 16040–16045. <https://doi.org/10.1073/pnas.0903446106>.
- Hublin, J.-J., 2015. The modern human colonization of western Eurasia: when and where? *Quat. Sci. Rev.* 118, 194–210. <https://doi.org/10.1016/j.quascirev.2014.08.011>.
- Hublin, J.-J., Sirakov, N., Aldeias, V., Bailey, S., Bard, E., Delvigne, V., Endarova, E., Fagault, Y., Fewlass, H., Hajdinjak, M., Kromer, B., Krumov, I., Marreiros, J., Martisius, N.L., Paskulin, L., Sinet-Mathiot, V., Meyer, M., Pääbo, S., Popov, V., Rezek, Z., Sirakova, S., Skinner, M.M., Smith, G.M., Spasov, R., Talamo, S., Tuna, T., Wacker, L., Welker, F., Wilcke, A., Zahariev, N., McPherron, S.P., Tsanova, T., 2020. Initial upper palaeolithic Homo sapiens from Bacho Kiro cave, Bulgaria. *Nature* 581, 299–302. <https://doi.org/10.1038/s41586-020-2259-z>.
- Inizan, M.L., Reduron-Ballinger, M., Roche, H., Tixier, J., 1995. *Technologie de la pierre taillée. Préhistoire de la pierre taillée. Cercle de recherches et d'études préhistoriques*. Meudon.
- Kuhn, S.L., 2020. *The Evolution of Paleolithic Technologies*. Routledge, Oxon and New York (Routledge, Oxon and New York).
- Kuhn, S.L., 1991. “Unpacking” reduction: lithic raw material economy in the moustierian of west-Central Italy. *J. Anthropol. Res.* 10, 76–106. [https://doi.org/10.1016/0278-4165\(91\)90022-4](https://doi.org/10.1016/0278-4165(91)90022-4).
- Kuhn, S.L., 1990. A geometric Index of reduction for unifacial stone tools. *J. Archaeol. Sci.* 17, 583–593.
- Kuhn, S.L., Shmelmitz, R., 2023. From hafting to retouching: miniaturization as tolerance control in paleolithic and neolithic blade production. *J. Archaeol. Method Theor.* 30, 678–701. <https://doi.org/10.1007/s10816-022-09575-5>.
- Le Brun-Ricalens, F., 2005. *Chronique d'une reconnaissance attendue. Outils "carénés", outils "ncléiformes": noyaux à lamelles. Bilan après un siècle de recherches typologiques, technologiques et tracéologiques*. In: Le Brun-Ricalens, F. (Ed.), *Productions Lamellaires Attribuées à l'Aurignacien*. MNHA, Luxembourg, pp. 23–72.
- Lombao, D., 2021. Reducción y gestión volumétrica: aproximación a la variabilidad y evolución de las dinámicas de explotación durante el Pleistoceno inferior y medio europeo, a través de los conjuntos de Gran Dolina y Galería (Sierra de Atapuerca, Burgos) y de El Barranc d. Universitat Rovira i Virgili, Tarragona.
- Lombao, D., Cuevas-Temprana, A., Mosquera, M., Morales, J.I., 2020. A new approach to measure reduction intensity on cores and tools on cobbles: the Volumetric Reconstruction Method. *Archaeol. Anthropol. Sci.* 12 <https://doi.org/10.1007/s12520-020-01154-7>.
- Lombao, D., Cuevas-Temprana, A., Rabuñal, J.R., Morales, J.I., Mosquera, M., 2019. The effects of blank size and knapping strategy on the estimation of core's reduction intensity. *Archaeol. Anthropol. Sci.* 11, 5445–5461. <https://doi.org/10.1007/s12520-019-00879-4>.
- Lombao, D., Falucci, A., Moos, E., Peresani, M., 2023a. Research compendium for “Unravelling technological behaviors through core reduction intensity. The case of the early Protoaurignacian assemblage from Fumane Cave.” Zenodo. <https://doi.org/10.5281/zenodo.8212572>.
- Lombao, D., Rabuñal, J.R., Cuevas-Temprana, A., Mosquera, M., Morales, J.I., 2023b. Establishing a new workflow in the study of core reduction intensity and distribution. *J. Lit. Stud.* 10, 25. <https://doi.org/10.2218/jls.7257>.
- Lombao, D., Rabuñal, J.R., Morales, J.I., Ollé, A., Carbonell, E., Mosquera, M., 2023c. The technological behaviours of Homo antecessor: core management and reduction intensity at Gran Dolina-td6.2 (Atapuerca, Spain). *J. Archaeol. Method Theor.* 30, 964–1001. <https://doi.org/10.1007/s10816-022-09579-1>.
- Maillo-Fernández, J.M., 2005. La producción lamellaire de l'Aurignacien de la grotte Morín (Cantabrie, Espagne). In: Le Brun-Ricalens, F. (Ed.), *Productions Lamellaires Attribuées à l'Aurignacien: Chaînes Opératoires et Perspectives Technoculturelles*. MNHA, Luxembourg, pp. 339–357.
- Marciani, G., Ronchitelli, A., Arrighi, S., Badino, F., Bortolini, E., Boscato, P., Boschin, F., Crezzini, J., Delpiano, D., Falucci, A., Figus, C., Lugli, F., Oxilia, G., Romandini, M., Riel-Salvatore, J., Negrino, F., Peresani, M., Spinapolic, E.E., Moroni, A., Benazzi, S., 2020. Lithic techno-complexes in Italy from 50 to 39 thousand years BP: an overview of lithic technological changes across the Middle-Upper Palaeolithic boundary. *Quat. Int.* 551, 123–149. <https://doi.org/10.1016/j.quaint.2019.11.005>.
- Mellars, P., 2006. Archeology and the dispersal of modern humans in Europe: deconstructing the “aurignacian”. *Evol. Anthropol. Issues News Rev.* 15, 167–182. <https://doi.org/10.1002/evan.20103>.
- Morales, J.I., 2016. Distribution patterns of stone-tool reduction: establishing frames of reference to approximate occupational features and formation processes in Paleolithic societies. *J. Anthropol. Archaeol.* 41, 231–245. <https://doi.org/10.1016/j.jaa.2016.01.004>.
- Morales, J.I., Lorenzo, C., Vergès, J.M., 2015. Measuring retouch intensity in lithic tools: a new proposal using 3D scan data. *J. Archaeol. Method Theor.* 22, 543–558. <https://doi.org/10.1007/s10816-013-9189-0>.
- Muller, A., Clarkson, C., Baird, D., Fairbairn, A., 2018. Reduction intensity of backed blades: bulk consumption, regularity and efficiency at the early Neolithic site of Boncuklu, Turkey. *J. Archaeol. Sci. Reports* 21, 721–732. <https://doi.org/10.1016/j.jasrep.2018.08.042>.
- Nelson, M.C., 1991. *The study of technological organization*. Archaeol. Method Theor. 3, 57–100.
- Nigst, P.R., Haesaerts, P., Damblon, F., Frank-Fellner, C., Mallol, C., Viola, B., Götzinger, M., Niven, L., Trnka, G., Hublin, J.-J., 2014. Early modern human settlement of Europe north of the Alps occurred 43,500 years ago in a cold steppe-type environment. *Proc. Natl. Acad. Sci. USA* 111, 14394–14399. <https://doi.org/10.1073/pnas.1412201111>.
- Normand, C., O'Farrell, M., Rios-Garaizar, J., 2008. Quelle(s) utilisation(s) pour les productions lamellaires de l'Aurignacien Archaique? Quelques données et réflexions à partir des exemplaires de la grotte d'Isturiz (Pyrénées-Atlantiques; France). *Palethnologie* 1, 7–46.
- Ortega-Cobos, D., Soler, N., Maroto, J., 2005. La producción de lamellas pendant l'Aurignacien archaïque dans la grotte de l'Arbreda: organisation de la production, variabilité des méthodes et des objectifs. In: Le Brun-Ricalens, F. (Ed.), *Productions Lamellaires Attribuées à l'Aurignacien*. MNHA, Luxembourg, pp. 359–373.
- Otte, M., 2013. *Les Gravettiens*. Éditions Errance, Paris.
- Pargeter, J., Shea, J.J., 2019. Going big versus going small: lithic miniaturization in hominin lithic technology. *Evol. Anthropol. Issues News Rev.* 28, 72–85. <https://doi.org/10.1002/evan.21775>.
- Pasha, G.R., Khan, S.M., Pasha, A.H., 2006. Empirical analysis of the Weibull distribution for failure data. *J. Stat.* 13, 33–45.
- Peresani, M., 2022. Inspecting human evolution from a cave. Late Neanderthals and early sapiens at Grotta di Fumane: present state and outlook. *J. Anthropol. Sci.* 100, 71–107. <https://doi.org/10.4436/JASS.10016>.
- Peresani, M., 2012. Fifty thousand years of flint knapping and tool shaping across the Mousterian and Uluzzian sequence of Fumane cave. *Quat. Int.* 247, 125–150. <https://doi.org/10.1016/j.quaint.2011.02.006>.
- Peresani, M., Cremaschi, M., Ferraro, F., Falguères, C., Bahain, J.-J., Gruppioni, G., Sibilia, E., Quarta, G., Calcagnile, L., Dolo, J.-M., 2008. Age of the final middle palaeolithic and uluzzian levels at Fumane cave, northern Italy, using 14C, ESR, 234U/230Th and thermoluminescence methods. *J. Archaeol. Sci.* 35, 2986–2996. <https://doi.org/10.1016/j.jas.2008.06.013>.
- Peresani, M., Cristiani, E., Romandini, M., 2016. The uluzzian technology of grotta di Fumane and its implication for reconstructing cultural dynamics in the middle-upper palaeolithic transition of western Eurasia. *J. Hum. Evol.* 91, 36–56. <https://doi.org/10.1016/j.jhevol.2015.10.012>.
- Peresani, M., Forte, M., Quaggiotto, E., Colonese, A.C., Romandini, M., Cilli, C., Giacobini, G., 2019. Marine and freshwater shell exploitation in the early upper paleolithic: Re-examination of the assemblages from Fumane cave (NE Italy). *PaleoAnthropology* 64–81. <https://doi.org/10.4207/PA.2019.ART124>.
- Peyrony, D., 1933. Les industries “aurignaciennes” dans le bassin de la Vézère. *Bull. la Société Préhistorique Française* 543–559.
- Pigeot, N., 1987. Magdaléniens d’Étoliennes. *Economie de débitage et organisation sociale*. CNRS Editions, Paris.
- Porraz, G., Simon, P., Pasquini, A., 2010. Identité technique et comportements économiques des groupes proto-aurignaciens à la grotte de l’Observatoire (principauté de Monaco). *Gall. Prehist.* 52, 33–59.
- Posit team, 2023. RStudio. Integrated Development Environment for R. PBC, Boston, MA.
- R Core Team, 2022. R: A Language and Environment for Statistical Computing (Vienna, Austria).
- Rabuñal, J.R., 2016. La tecnología lítica del Magdaleniense Superior Final de la Cova de Les Borres (La Febró): estudio morfológico y definición de estrategias de explotación. Master Thesis. Univ. Rovira i Virgili.
- Riel-Salvatore, J., Negrino, F., 2018. Proto-aurignacian lithic technology, mobility, and human niche construction: a case study from riparo Bombrini, Italy. In: Robinson, E., Sellet, F. (Eds.), *Lithic Technological Organization and Paleoenvironmental Change*. Springer, NY, pp. 163–187. https://doi.org/10.1007/978-3-319-64407-3_8.
- Rios-Garaizar, J., 2012. Industria lítica y sociedad del paleolítico medio al superior en torno al Golfo de Bizkaia. PUBLICAN, Ediciones de la Universidad de Cantabria, Santander.

- Rolland, N., Dibble, H.L., 1990. A new synthesis of Middle Palaeolithic variability. *Am. Antiq.* 55, 480–499.
- Romagnoli, F., Vaquero, M., 2019. The challenges of applying refitting analysis in the Palaeolithic archaeology of the twenty-first century: an actualised overview and future perspectives. *Archaeol. Anthropol. Sci.* 11, 4387–4396. <https://doi.org/10.1007/s12520-019-00888-3>.
- Sánchez-Martínez, J., Roda Gilabert, X., Vega Bolívar, S., Martínez-Moreno, J., Benito-Calvo, A., Mora Torcal, R., 2022. Beyond shapes: core reduction strategies in the magdalenian of cova gran de Santa linya (NE Iberia). *J. Paleolit. Archaeol.* 5, 7. <https://doi.org/10.1007/s41982-022-00115-x>.
- Santamaría, D., 2012. La transición del Paleolítico medio al superior en Asturias. In: *El Abrigo de La Viña (La Manzaneda, Oviedo) y la Cueva de El Sidrón (Borines, Piloña)*. Servicio de Publicaciones de la Universidad de Oviedo, Oviedo.
- Schiffer, M.B., 1987. Formation Processes of the Archaeological Record. University of New Mexico Press, Albuquerque.
- Shott, M.J., 2002. Weibull estimation on use life distribution in experimental spear-point data. *Lithic Technol.* 27, 93–109. <https://doi.org/10.1080/01977261.2002.11720993>.
- Shott, M.J., Sillito, P., 2005. Use life and curation in New Guinea experimental used flakes. *J. Archaeol. Sci.* 32, 653–663. <https://doi.org/10.1016/j.jas.2004.11.012>.
- Shott, M.J., Sillito, P., 2004. Modeling use-life distributions in archaeology using new Guinea wola ethnographic data. *Am. Antiq.* 69, 339–355. <https://doi.org/10.2307/4128424>.
- Slimak, L., Zanolli, C., Higham, T., Frouin, M., Schwenninger, J.-L., Arnold, L.J., Demuro, M., Douka, K., Mercier, N., Guérin, G., Valladas, H., Yvorra, P., Giraud, Y., Seguin-Orlando, A., Orlando, L., Lewis, J.E., Muth, X., Camus, H., Vandeveld, S., Buckley, M., Mallol, C., Stringer, C., Metz, L., 2022. Modern human incursion into Neanderthal territories 54,000 years ago at Mandrin. *France. Sci. Adv.* 8 <https://doi.org/10.1126/sciadv.abj9496>.
- Tainter, M.C., 1999. Palaeolithic mollusc exploitation at riparo Mochi (balzi rossi, Italy): food and ornaments from the aurignacian through epigravettian. *Antiquity* 73, 735–754. <https://doi.org/10.1017/S0003598X00065492>.
- Szmidt, C.C., Brou, L., Jaccotey, L., 2010. Direct radiocarbon (AMS) dating of split-based points from the (Proto)Aurignacian of Trou de la Mère Clochette, Northeastern France. Implications for the characterization of the Aurignacian and the timing of technical innovations in Europe. *J. Archaeol. Sci.* 37, 3320–3337. <https://doi.org/10.1016/j.jas.2010.08.001>.
- Tafelmaier, I., 2017. Technological Variability at the Beginning of the Aurignacian in Northern Spain. *Wissenschaftliche Schriften des Neanderthal Museums, Mettmann*.
- Teyssandier, N., 2007. En route vers l'Ouest. Les débuts de l'Aurignacien en Europe. *John and Erica Hedges, Oxford*.
- Teyssandier, N., Bon, F., Bordes, J.-G., 2010. Within projectile range: some thoughts on the appearance of the aurignacian in Europe. *J. Anthropol. Res.* 66, 209–229. <http://www.jstor.org/stable/27820882>.
- Teyssandier, N., Zilhão, J., 2018. On the entity and antiquity of the aurignacian at willendorf (Austria): implications for modern human emergence in Europe. *J. Paleolit. Archaeol.* 1, 107–138. <https://doi.org/10.1007/s41982-017-0004-4>.
- Tsanova, T., Zwyns, N., Eizenberg, L., Teyssandier, N., Le Brun-Ricalens, F., Otte, M., 2012. Le plus petit dénominateur commun : réflexion sur la variabilité des ensembles lamellaires du Paléolithique supérieur ancien d'Eurasie. Un bilan autour des exemples de Kozarnika (Est des Balkans) et Yafteh (Zagros central). *Anthropologie* 116, 469–509. <https://doi.org/10.1016/j.anthro.2011.10.005>.
- Valdes, V.C., Bischoff, J.L., 1989. Accelerator 14C dates for early upper paleolithic (basal Aurignacian) at El Castillo Cave (Spain). *J. Archaeol. Sci.* 16, 577–584. [https://doi.org/10.1016/0305-4403\(89\)90023-X](https://doi.org/10.1016/0305-4403(89)90023-X).
- Vanhaeften, M., D'Errico, F., 2006. Aurignacian ethno-linguistic geography of Europe revealed by personal ornaments. *J. Archaeol. Sci.* 33, 1105–1128. <https://doi.org/10.1016/j.jas.2005.11.017>.
- Verma, C., Dujardin, V., Trinkaus, E., 2012. The early aurignacian human remains from La quina-aval (France). *J. Hum. Evol.* 62, 605–617. <https://doi.org/10.1016/j.jhevol.2012.02.001>.
- Villaverde, V., Sanchis, A., Badal, E., Bel, M.Á., Bergadà, M.M., Eixea, A., Guillem, P.M., Martínez-Alfaró, Á., Martínez-Valle, R., Martínez-Varea, C.M., Real, C., Steier, P., Wild, E.M., 2021. Cova de les Mallades (Valencia, Spain): new Insights About the Early Upper Palaeolithic in the Mediterranean Basin of the Iberian Peninsula. *J. Paleolit. Archaeol.* 4, 5. <https://doi.org/10.1007/s41982-021-00081-w>.
- Wickham, H., 2016. *ggplot2: Elegant Graphics for Data Analysis*. Springer-Verlag, New York.
- Wickham, H., 2011. The split-apply-combine strategy for data analysis. *J. Stat. Software* 40, 1–29.
- Wickham, H., 2007. Reshaping data with the reshape package. *J. Stat. Software* 21, 1–20.
- Wickham, H., François, R., Henry, L., Müller, K., Vaughan, D., 2023. *Dplyr: A Grammar of Data Manipulation*.
- Wood, R.E., Arrizabalaga, A., Camps, M., Fallon, S., Iriarte-Chiapusso, M.-J., Jones, R., Maroto, J., de la Rasilla, M., Santamaría, D., Soler, J., Soler, N., Villaluenga, A., Higham, T.F.G., 2014. The chronology of the earliest upper palaeolithic in northern iberia: new insights from L'Arbreda, Labeko Koba and La Viña. *J. Hum. Evol.* 69, 91–109. <https://doi.org/10.1016/j.jhevol.2013.12.017>.
- Yezzi-Woodley, K., Calder, J., Olver, P.J., Cody, P., Huffstutler, T., Terwilliger, A., Melton, J.A., Tappen, M., Coil, R., Tostevin, G., 2021. The virtual goniometer: demonstrating a new method for measuring angles on archaeological materials using fragmentary bone. *Archaeol. Anthropol. Sci.* 13, 106. <https://doi.org/10.1007/s12520-021-01335-y>.
- Zilhão, J., D'Errico, F., 2003. An Aurignacian «garden of Eden» in Southern Germany ? an Alternative Interpretation of the Geissenklosterle and a Critique of the Kulturpumpe Model. *Paléo*. <https://doi.org/10.4000/paleo.1231>.